การปรับปรุงภาพถ่ายเหนือเสียงโดยวิธีการแปรผัน

นายวัชชิราวุฒิ ศรีโคตร

วิทยานิพนธ์นี้เป็นส่วนหนึ่งของการศึกษาตามหลักสูตรปริญญาวิทยาศาสตรมหาบัณฑิต

สาขาวิชาคณิตศาสตร์ประยุกต์

มหาวิทยาลัยเทคโนโลยีสุรนารี

ปีการศึกษา 2551

ULTRASOUND IMAGE ENHANCEMENT BY MEANS OF A VARIATIONAL APPROACH

WATCHIRAWOOT SEEKOT

A Thesis Submitted in Partial Fulfillment of the Requirements for the Degree of Master of Science in Applied Mathematics

Suranaree University of Technology

Academic Year 2008

ULTRASOUND IMAGE ENHANCEMENT BY MEANS OF A VARIATIONAL APPROACH

Suranaree University of Technology has approved this thesis submitted in partial fulfillment of the requirements for a Master's Degree.

Thesis Examining Committee

(Assoc. Prof. Dr. Prapasri Asawakun)
Chairperson

(Asst. Prof. Dr. Jessada Tanthanuch)
Member (Thesis Advisor)

(Asst. Prof. Dr. Eckart Schulz)
Member

(Dr. Paramate Horkaew)
Member

(Prof. Dr. Pairote Sattayatham)
Vice Rector for Academic Affairs

(Assoc. Prof. Dr. Prapan Manyum)
Dean of Institute of Science

วัชชิราวุฒิ ศรีโคตร : การปรับปรุงภาพถ่ายเหนือเสียงโดยวิธีการแปรผัน (ULTRASOUND IMAGE ENHANCEMENT BY MEANS OF A VARIATIONAL APPROACH)
อาจารย์ที่ปรึกษา : ผศ. ดร. เจษฎา ตัณฑนุช, 72 หน้า.

เมื่อคลื่นเหนือเสียงตกกระทบที่พื้นผิวหยาบจะทำให้เกิดการกระเจิงและสัญญาณรบกวนที่เรียกว่า สเปกเคิล ในภาพถ่ายเหนือเสียง โดยที่การเกิดสัญญาณรบกวนแบบสเปกเคิลนั้น สามารถอธิบายได้ด้วยการแจกแจงทางสถิติที่เรียกว่า การแจกแจงเรย์ลี ซึ่งมีฟังก์ชันการแจกแจงความน่าจะเป็น ดังนี้

$$P(r) = \frac{r}{\sigma^2} e^{-r^2/(2\sigma^2)}$$

เมื่อ r มากกว่าหรือเท่ากับศูนย์ และ σ คือพารามิเตอร์ โดยตัวแบบทางคณิตศาสตร์ที่ใช้สำหรับการปรับปรุงภาพของภาพถ่ายเหนือเสียงที่มีสัญญาณรบกวนสามารถแสดงได้โดยสมการเชิงปริพันธ์ดังนี้

$$E(u) = \beta \iint_{\Omega} \left(\sqrt{u_x^2 + u_y^2} \right) dxdy + \iint_{\Omega} \left(\frac{\tilde{u}^2}{u^2} + 2\ln u + \mathrm{F}(\tilde{u}) \right) dxdy$$

เมื่อ $u(x, y)$ คือค่าของความเข้มสี ณ ตำแหน่ง (x, y) ของภาพที่ต้องการ $\tilde{u}(x, y)$ คือค่าของความเข้มสี ณ ตำแหน่ง (x, y) ของภาพที่กำลังพิจารณา Ω คือโดเมนของภาพ และ F เป็นค่าคงที่ซึ่งขึ้นกับ $\tilde{u}(x, y)$

แคลคูลัสของการแปรผันเป็นเครื่องมือที่ใช้ในการหาคำตอบ u ที่เหมาะสมที่สุดของสมการเชิงปริพันธ์ โดยจะแปลงสมการเชิงปริพันธ์ไปสู่สมการเชิงอนุพันธ์ ดังนี้

$$\frac{\partial}{\partial x}\left(\frac{u_x}{\sqrt{u_x^2 + u_y^2}} \right) + \frac{\partial}{\partial y}\left(\frac{u_y}{\sqrt{u_x^2 + u_y^2}} \right) + \frac{2}{\beta u^3}\left(\tilde{u}^2 - u^2 \right) = 0$$

โดยจะเรียกสมการนี้ว่า สมการออยเลอร์-ลากรองจ์ และคำตอบ u นั้นจะเป็นภาพที่ไม่มีสัญญาณรบกวน สำหรับการหาคำตอบสมการออยเลอร์-ลากรองจ์ในโปรแกรมคอมพิวเตอร์ต้นแบบจะใช้วิธีเชิงตัวเลขที่เรียกว่า วิธีเกรเดียนท์เดสเซนท์ และผลลัพธ์ที่ได้แสดงให้เห็นว่าสัญญาณรบกวนในภาพถ่ายเหนือเสียงทั้งแบบภาพนิ่งและภาพวีดิทัศน์มีปริมาณที่ลดลง

สาขาวิชาคณิตศาสตร์ ลายมือชื่อนักศึกษา_____

ปีการศึกษา 2551 ลายมือชื่ออาจารย์ที่ปรึกษา_____

ลายมือชื่ออาจารย์ที่ปรึกษาร่วม_____

WATCHIRAWOOT SEEKOT : ULTRASOUND IMAGE ENHANCEMENT BY MEANS OF A VARIATIONAL APPROACH. THESIS ADVISOR : ASST. PROF. JESSADA TANTHANUCH, Ph.D. 72 PP.

CALCULUS OF VARIATIONS / EULER-LAGRANGE EQUATION/ GRADIENT DESCENT METHOD/ RAYLEIGH DISTRIBUTION / SPECKLE NOISE / TOTAL VARIATIONS / ULTRASOUND IMAGE / VARIATIONAL APPROACH

When ultrasonic wave encounter rough surfaces, they become scattered, leading to speckle noise in an ultrasound image. The speckle noise occurring can be explained statistically by the Rayleigh distribution:

$$R_\sigma(r) = \frac{r}{\sigma^2} e^{-\frac{r^2}{2\sigma^2}},$$

where $r \geq 0$ and σ is a parameter.

One mathematical model for reconstructing an observed noisy ultrasound image is the integral equation

$$E(u) = \beta \iint_\Omega \left(\sqrt{u_x^2 + u_y^2} \right) dA + \iint_\Omega \left(\frac{\widetilde{u}^2}{u^2} + 2 \ln u + \mathcal{F}(\widetilde{u}) \right) dA,$$

where $\mathcal{F}(\widetilde{u})$ being a constant depending on $\widetilde{u}$, for coordinate (x, y), $u(x, y)$ is intensity of desired image, $\widetilde{u}(x, y)$ is intensity of observed image and Ω is the image domain.

The Calculus of Variations is the tool used to finding an optimal solution u of the integral equation. It transforms the integral equation to the differential equation

$$\frac{\partial}{\partial x} \left(\frac{u_x}{\sqrt{u_x^2 + u_y^2}} \right) + \frac{\partial}{\partial y} \left(\frac{u_y}{\sqrt{u_x^2 + u_y^2}} \right) + \frac{2}{\beta u^3} (\widetilde{u}^2 - u^2) = 0,$$

where $u = \widetilde{u}$ on $\partial\Omega$, which is called Euler-Lagrange equation.

The solution u is expected to be the noiseless image. The gradient descent method is used to find the solution of the Euler-Lagrange equation numerically in the prototype software. The results show that the noise in the ultrasound images and videos is reduced.

School of Mathematics

Academic Year 2008

Student's Signature _____

Advisor's Signature _____

Co-Advisor's Signature _____

ACKNOWLEDGEMENTS

I would like to express my sincere gratitude to my thesis advisor, Asst. Prof. Dr. Jessada Tanthanuch and thesis co-advisor, Dr. Paramate Horkaew, for their support, patient help, providing me with extensive literature background and offering many useful suggestions. Also, I am indebted Dr. Chumrus Sakulpaisarn for his ultrasound videos.

In addition, I would like to acknowledge the personal and professional support received from the faculty of the School of Mathematics, Suranaree University of Technology: Assoc. Prof. Dr. Prapasri Asawakun, Prof. Dr. Sergey Meleshko, Prof. Dr. Pairote Sattayatham, Assoc. Prof. Dr. Nikolay Moshkin, Asst. Prof. Dr. Arjuna Chaiyasena, and Asst. Prof. Dr. Eckart Schulz.

Watchirawoot Seekot

CONTENTS

Page

ABSTRACT IN THAI I

ABSTRACT IN ENGLISH II

ACKNOWLEDGEMENTS IV

CONTENTS V

LIST OF TABLES VII

LIST OF FIGURES VIII

CHAPTER

I INTRODUCTION 1

II RAYLEIGH DISTRIBUTION AND SPECKLE NOISE . . . 4

2.1 Rayleigh distribution 4

2.2 Derivation of the Rayleigh probability density function 4

2.3 Harmonic Waves 6

2.3.1 One-Dimensional Waves and Harmonic Waves 6

2.3.2 Superposition of harmonic Waves of the Same Frequency . . 7

2.3.3 Coherence and Incoherence 11

2.4 Speckle 12

III CALCULUS OF VARIATIONS AND ROF MODEL 15

3.1 Calculus of Variations 15

3.2 The ROF Model 17

3.2.1 Gradient 18

3.2.2 The Least Square Problem 19

CONTENTS (Continued)

Page

3.2.3 Description of the ROF Model 20

IV RESULT AND CONCLUSION 23

4.1 Description of the Proposed Model 23

4.2 Existence and Uniqueness 27

4.3 Numerical Scheme 35

4.4 Numerical Results 36

4.5 Conclusion 48

REFERENCES 50

APPENDICES

APPENDIX A SPECKLE FILTERS IN RADAR IMAGING 54

APPENDIX B PROTOTYPE SOFTWARE 57

B.1 Prototype Software 57

B.2 Source Code 58

CURRICULUM VITAE 72

LIST OF TABLES

Table		Page
4.1	Correlation coefficients of reconstructed pattern images	37
4.2	Correlation coefficients of reconstructed Lenna images.	38

LIST OF FIGURES

Figure		Page
2.1	The figures of coherent waves	12
2.2	The figure of waves that combine with lots of different phases nearly cancel out and yield very low irradiance (incoherent).	12
2.3	Figure of scattering reflection from a rough surface.	13
4.1	The figures of pattern images reconstructed by ROF model.	39
4.2	The figures of pattern images reconstructed by Le et al.'s model . .	40
4.3	The figures of pattern images reconstructed by Proposed model. . .	41
4.4	The figures of Lenna images reconstructed by ROF model.	42
4.5	The figures of Lenna images reconstructed by Le et al.'s model. . .	43
4.6	The figures of Lenna images reconstructed by proposed model. . . .	44
4.7	The figures of ultrasound images reconstructed by ROF model. . .	45
4.8	The figures of ultrasound images reconstructed by Le et al.'s model.	46
4.9	The figures of ultrasound images reconstructed by proposed model.	47
B.1	The figure of prototype software and its components.	57

CHAPTER I

INTRODUCTION

Ultrasound images provide clinicians with non-invasive, low cost and real-time images which can help them in diagnosis, planning and therapy. However, the ultrasonic wave encounters rough surfaces which results in scattering and leads to noise which is called speckle noise.

According to the literature review, there are many researches concerned with speckle filters for radar images. For example the filter by *Frost et al.*, the filter by *Lee*, the filter by *Kuan et al.* and the *homomorphic filter*.

Frost et al. describe a filter dealing with multiplicative noise model while the additive noise model is used in the filter by Kuan et al. Moreover, Lee adapted the linear filter to consider the multiplicative noise model, while the homomorphic filter uses the logarithm function to transform the multiplicative noise model to the linear filter. The method of *minimum mean square error* is used for these filters. See more details of all of these filter in APPENDIX A.

The main disadvantage of the above filters is that we have to know the information of the noise in the computation. Difficulties arise when we work with an ultrasound video because we do not have the speckle noise information.

This problem can be solved by the mathematical model called the *variational approach*. The representation of the image in several variational models is presented by

$$\widetilde{u}(x,y) = u(x,y) + n(x,y),$$

where (x,y) is the spatial coordinate, $u(x,y)$ is intensity of the desired image at

coordinate (x, y), $\widetilde{u}(x, y)$ is the intensity of the observed image and $n(x, y)$ is the intensity of additive noise at coordinate (x, y). The variational approach is used for finding the desired image u from the obtained image $\widetilde{u}$.

There are studies of digital image denoising models dealing with the variational approach, for example

1. **The ROF model (1992)**

   In 1992, Rudin, Osher, and Fatemi presented a mathematical denoising model which is called the ROF model which uses the additive noise model and is based on calculus of variation. The ROF model considers u as the solution to a problem of calculus of variation which minimizes the functional

   $$F(u) = \iint\limits_{\Omega} \left(\sqrt{u_x^2 + u_y^2}\right) dA + \lambda \iint\limits_{\Omega} (u - \widetilde{u})^2 dA,$$

   where $\Omega \in \mathbb{R}^2$ is the domain of the image functions and λ is a chosen parameter. By calculus of variations, the solution of this problem is obtained when the Euler-Lagrange differential equation is satisfied, i.e.

   $$\frac{\partial}{\partial x}\left(\frac{u_x}{\sqrt{u_x^2 + u_y^2}}\right) + \frac{\partial}{\partial y}\left(\frac{u_y}{\sqrt{u_x^2 + u_y^2}}\right) + \lambda(u - \widetilde{u}) = 0,$$

   where $\dfrac{\partial u}{\partial N} = 0$ on $\partial\Omega$ and N is the normal vector to the boundary $\partial\Omega$.

2. **The variational approach for Poisson noise (2007)**

   Le, Chatrand and Asaki adapted the ROF model to reduce Poisson noise in the image by minimizing the functional

   $$G(u) = \beta \iint\limits_{\Omega} \left(\sqrt{u_x^2 + u_y^2}\right) dA + \iint\limits_{\Omega} (u - \widetilde{u} \ln u) dA.$$

   The Euler-Lagrange differential equation for solving this problem is

   $$\frac{\partial}{\partial x}\left(\frac{u_x}{\sqrt{u_x^2 + u_y^2}}\right) + \frac{\partial}{\partial y}\left(\frac{u_y}{\sqrt{u_x^2 + u_y^2}}\right) + \frac{1}{\beta u}(u - \widetilde{u}) = 0,$$

   where $\dfrac{\partial u}{\partial N} = 0$ on $\partial\Omega$ and N is the normal vector to the boundary $\partial\Omega$.

In this thesis, a variational approach adapted from the ROF model is used to construct the model to reduce the speckle noise in the ultrasound image. The model is to minimize the functional

$$E(u) = \beta \iint_{\Omega} \left(\sqrt{u_x^2 + u_y^2} \right) dA + \iint_{\Omega} \left(\frac{\widetilde{u}^2}{u^2} + 2 \ln u + \mathcal{F}(\widetilde{u}) \right) dA,$$

where β is a chosen parameter and $\mathcal{F}(\widetilde{u})$ is a function of $\widetilde{u}$. We show that this minimization problem has a unique solution.

Here, the Euler-Lagrange equation for minimizing $E(u)$ is

$$\frac{\partial}{\partial x} \left(\frac{u_x}{\sqrt{u_x^2 + u_y^2}} \right) + \frac{\partial}{\partial y} \left(\frac{u_y}{\sqrt{u_x^2 + u_y^2}} \right) + \frac{2}{\beta u^3} (\widetilde{u}^2 - u^2) = 0,$$

where $u = \widetilde{u}$ on $\partial\Omega$.

The solution of the above problem is approximated by the numerical method called *gradient descent method*. Furthermore, prototype software for the model implementation is developed . The pattern image and the Lenna image are used to evaluate the proposed model by comparing the *correlation coefficient* of the noisy images and the reconstructed images to the original ones. It is found that the model can be used to denoise noisy images and ultrasound videos. The description of the results is shown in section 4.4.

CHAPTER II

RAYLEIGH DISTRIBUTION AND SPECKLE NOISE

This chapter presents the mathematical background of speckle noise which concerns with the Rayleigh distribution.

2.1 Rayleigh distribution

The *Rayleigh distribution* is a continuous probability distribution. It can arise when a two-dimensional vector has elements that are normally distributed random variables, independent and they both have zero mean and equal variance. The vector's magnitude will then have a Rayleigh distribution.

Definition 2.1. The **Rayleigh probability density function** is

$$R_\sigma(r) = \frac{r}{\sigma^2} e^{-\frac{r^2}{2\sigma^2}}, \tag{2.1}$$

where $r \geq 0$ and σ is parameter.

2.2 Derivation of the Rayleigh probability density function

Let $< x, y > \in \mathbb{R}^2$ be a two-dimensional vector where x and y are normally distributed random variables, independent and both having zero mean and equal variance. By definition of normal distribution, the probability density of the random variable x is

$$N_\sigma(x) = \frac{1}{\sigma\sqrt{2\pi}} e^{-\frac{x^2}{2\sigma^2}},$$

where σ is a variance.

Similarly, the probability density of the random variable y is

$$N_\sigma(y) = \frac{1}{\sigma\sqrt{2\pi}} e^{-\frac{y^2}{2\sigma^2}}.$$

Since x and y are independent then, the probability density function in the rectangular coordinate of $< x, y >$ is

$$\begin{aligned} \widehat{R}(x,y) &= N_\sigma(x) N_\sigma(y) \\ &= \frac{1}{2\pi\sigma^2} e^{-\frac{(x^2+y^2)}{2\sigma^2}}. \end{aligned}$$

We have the joint distribution in rectangular coordinates as

$$\int_{-\infty}^{\infty}\int_{-\infty}^{\infty} \widehat{R}(x,y)dxdy = \int_{-\infty}^{\infty}\int_{-\infty}^{\infty} \frac{1}{2\pi\sigma^2} e^{-\frac{(x^2+y^2)}{2\sigma^2}} dxdy.$$

By changing to the polar coordinate we let $x = r\cos\theta$ and $y = r\sin\theta$. The corresponding Jacobian is

$$\begin{vmatrix} \frac{\partial x}{\partial r} & \frac{\partial x}{\partial \theta} \\ \frac{\partial y}{\partial r} & \frac{\partial y}{\partial \theta} \end{vmatrix} = r.$$

By the theorem of changing variables to polar form (Wade, 1999) and property of distribution, we have

$$\int_{-\infty}^{\infty}\int_{-\infty}^{\infty} \frac{1}{2\pi\sigma^2} e^{-\frac{(x^2+y^2)}{2\sigma^2}} dxdy = \int_0^{2\pi}\int_0^{\infty} \frac{r}{2\pi\sigma^2} e^{-\frac{r^2}{2\sigma^2}} drd\theta = 1. \tag{2.2}$$

The marginal density function of r is obtained by integrating $\widehat{R}(r,\theta)$ with respect to θ, thus we get

$$\begin{aligned} \widehat{R}(r) &= \int_0^{2\pi} \frac{r}{2\pi\sigma^2} e^{-\frac{r^2}{2\sigma^2}} d\theta \\ &= \frac{r}{\sigma^2} e^{-\frac{r^2}{2\sigma^2}}. \end{aligned}$$

This function is known as the *Rayleigh density function* and

$$\mathcal{R}_\sigma(r) = \begin{cases} 0 & \text{if } r < 0 \\ \displaystyle\int_0^r \frac{\tau}{\sigma^2} e^{-\frac{\tau^2}{2\sigma^2}} d\tau & \text{if } r \geq 0 \end{cases}$$

is a Rayleigh distribution.

The notation $R_\sigma(r) = \frac{r}{\sigma^2} e^{-\frac{r^2}{2\sigma^2}}$ is denoted for the Rayleigh density function in this thesis.

2.3 Harmonic Waves

2.3.1 One-Dimensional Waves and Harmonic Waves

First, we will describe the mathematical expression for wave motion and the harmonic wave.

Definition 2.2. Let ψ be an n-dimensional vector, say $\psi = \psi(x_1, x_2, ..., x_n)$. The **Laplacian** $\nabla^2\psi$ of ψ is defined by

$$\nabla^2\psi = \frac{\partial^2\psi}{\partial x_1^2} + \frac{\partial^2\psi}{\partial x_2^2} + ... + \frac{\partial^2\psi}{\partial x_n^2}.$$

Note that we may sometimes replace x_n with variable t.

Definition 2.3. The **differential wave equation** which describes propagation of waves with speed v respect to time t is given by

$$\nabla^2\psi = \frac{1}{v^2}\frac{\partial^2\psi}{\partial t^2}.$$

In particular, the **one-dimensional differential wave equation** is given by

$$\frac{\partial^2\psi}{\partial x^2} = \frac{1}{v^2}\frac{\partial^2\psi}{\partial t^2}.$$

Definition 2.4. A function $y = f(x \pm vt)$ is said to be a function of **one-dimensional wave** which moves along the x-axis at speed v relative to coordinate (x, y) if it satisfies the one-dimensional differential wave equation,

$$\frac{\partial^2 y}{\partial x^2} = \frac{1}{v^2}\frac{\partial^2 y}{\partial t^2}. \tag{2.3}$$

Definition 2.5. Harmonic wave is a particular wave which involves the sine function

$$y = A\sin[c(x \pm vt)]$$

or cosine function

$$y = A\cos[c(x \pm vt)],$$

where A and c are constants. Note that A is called the amplitude of the wave and can be assumed to be nonnegative.

We claim that $y = A\sin[c(x \pm vt)]$ satisfies the one-dimensional differential wave equation. Since

$$\frac{\partial^2 y}{\partial x^2} = -Ac^2\sin[c(x \pm vt)]$$

and

$$\frac{\partial^2 y}{\partial t^2} = -Ac^2v^2\sin[c(x \pm vt)].$$

This shows that $y = A\sin[c(x \pm vt)]$ satisfies the one-dimensional differential wave equation, so it is a one-dimensional wave.

Similarly, in the case of $y = A\cos[c(x \pm vt)]$, we conclude that it is also a one-dimensional wave.

Denote $\omega = cv$ which is called the *angular frequency*. With these relationships, it is easy to show the equivalence of the following general forms for harmonic waves: $y = A\sin[cx \pm \omega t]$. Note that we only consider the case of the sine function because the case of the cosine function is similar.

2.3.2 Superposition of harmonic Waves of the Same Frequency

It is necessary to deal with situations in which two or more such waves arrive at the same point in space or exist together along the same direction. Several im-

portant cases of the combined effects of two or more harmonic waves are described in this section. The first case deals with the superposition of harmonic waves of different amplitudes and phases but with the same frequency. This leads to an important difference between the irradiance attainable from randomly phased and coherent harmonic waves.

To explain the combined effects of waves, we require the *superposition principle*[*].

By the superposition principle, the superposition of harmonic waves may be expressed in terms of equation

$$y = y_1 + y_2,$$

where y_1 and y_2 are the independent waves which exist together in the space.

The time variations of the harmonic waves at the given point can be expressed by

$$\begin{aligned} y_1 &= A_1 \sin(\omega t + \alpha_1), \\ y_2 &= A_2 \sin(\omega t + \alpha_2), \end{aligned}$$

where A_1, A_2 are amplitudes of y_1 and y_2, α_1, α_2 are phases of y_1 and y_2 respectively.

By the superposition principle, the resultant y_R at the point is

$$y_R = y_1 + y_2 = A_1 \sin(\omega t + \alpha_1) + A_2 \sin(\omega t + \alpha_2).$$

Using the trigonometric identity for sum of two sine functions with different angles and recombining terms,

$$y_R = (A_1 \cos\alpha_1 + A_2 \cos\alpha_2) \sin\omega t + (A_1 \sin\alpha_1 + A_2 \sin\alpha_2) \cos\omega t.$$

[*]The s*uperposition principle* says that "the resultant displacement is the sum of the separate displacements of the constituent waves".

Notice that if we set magnitude and phase angle as vectors and add them, a resultant or sum is found with magnitude A and phase α. The components of the resultant are

$$A\cos\alpha = A_1\cos\alpha_1 + A_2\cos\alpha_2$$

and

$$A\sin\alpha = A_1\sin\alpha_1 + A_2\sin\alpha_2.$$

The quantities A and α are defined by this technique, hence

$$y_R = A\cos\alpha\sin\omega t + A\sin\alpha\cos\omega t$$

or

$$y_R = A\sin(\omega t + \alpha).$$

We conclude that the resultant wave y_R is another harmonic wave of the same frequency ωt, with amplitude A and phase α. The cosine law may be applied to yield an expression for A,

$$A^2 = A_1^2 + A_2^2 + 2A_1A_2\cos(\alpha_2 - \alpha_1)$$

and the phase angle is given by

$$\alpha = \tan^{-1}\left(\frac{A_1\sin\alpha_1 + A_2\sin\alpha_2}{A_1\cos\alpha_1 + A_2\cos\alpha_2}\right).$$

Using induction, these computation generalize to the superposition of N harmonic waves:

$$y_k = A_k\sin(\omega t + \alpha_k)$$

of amplitude A_k and phase α_k. The resultant will be a wave

$$y_R = A\sin(\omega t + \alpha),$$

where

$$A\cos\alpha = A_1\cos\alpha_1 + A_2\cos\alpha_2 + ... + A_N\cos\alpha_N. \tag{2.4}$$

$$A\sin\alpha = A_1\sin\alpha_1 + A_2\sin\alpha_2 + ... + A_N\sin\alpha_N. \tag{2.5}$$

Thus,

$$\alpha = \tan^{-1}\left(\frac{\sum_{k=1}^{N} A_k\sin\alpha_k}{\sum_{k=1}^{N} A_k\cos\alpha_k}\right)$$

and by the Pythagorean theorem,

$$A^2 = \left(\sum_{k=1}^{N} A_k\sin\alpha_k\right)^2 + \left(\sum_{k=1}^{N} A_k\cos\alpha_k\right)^2.$$

The above equation may profitably be cast into a form that looks more like a generalization of the cosine law. Expanding each term, we have

$$A^2 = \sum_{k=1}^{N} A_k^2(\sin^2\alpha_k + \cos^2\alpha_k) + 2\sum_{k=1}^{N}\sum_{j>k}^{N} A_kA_j(\cos\alpha_k\cos\alpha_j + \sin\alpha_k\sin\alpha_j).$$

Note that the double sum represents all cross products, by the use of notation $j > k$ the self-product already accounted for in the first term and also avoiding a duplication of the indices.

Using the trigonometric identity of $\cos(\alpha_i - \alpha_j)$ in the second term, finally

$$A^2 = \sum_{k=1}^{N} A_k^2 + 2\sum_{k=1}^{N}\sum_{j>k}^{N} A_kA_j\cos(\alpha_k - \alpha_j). \tag{2.6}$$

The pair of equations (2.4) and (2.5) are easily express in exponential form. Each pair (A_k, α_k) uniquely determines a complex number

$$A_ke^{i\alpha_k} = A_k(\cos\alpha_k + i\sin\alpha_k).$$

Then the resultant wave is expressed by$Ae^{id} = A(\cos\alpha + i\sin\alpha)$.

Observe that by (2.4) and (2.5),

$$\begin{aligned} Ae^{i\alpha} &= A\cos\alpha + iA\sin\alpha \\ &= A\cos\alpha + iA\sin\alpha \\ &= \sum_{k=1}^{N} A_k\sin\alpha_k + i\sum_{k=1}^{N} A_k\sin\alpha_k \\ &= \sum_{k=1}^{N} A_ke^{i\alpha_k}. \end{aligned}$$

Summarizing, the sum of N harmonic waves of identical frequency is again a harmonic wave of the same frequency, with amplitude given by A and phase given by α.

2.3.3 Coherence and Incoherence

Before discussing speckle in the next section, *coherence* and *incoherence* are introduced. The term coherence and incoherence are used to describe the correlation between phases of *monochromatic waves*[†].

Definition 2.6. Let

$$\begin{aligned} y_1(x) &= A_1 \sin(\omega x + \alpha_1), \\ y_2(x) &= A_2 \sin(\omega x + \alpha_2) \end{aligned}$$

be harmonic waves with the same frequency ω. The **relative phase** of y_1 and y_2 is given by $\alpha_1 - \alpha_2$.

Definition 2.7. Waves are said to be **coherent** if they have a *constant relative phase*, which also implies that they have the same frequency. In the superposition of coherent waves, individual amplitudes add together. As present in figure 2.1(a) and 2.1(b), waves add constructively or subtract destructively, depending on their relative phase.

Definition 2.8. Waves are said to be **incoherent** if they have *random relative phase*, i.e. they are combined with a lots of different phases as shown in figure 2.2

[†]A **monochromatic wave** is represented by a wave function with harmonic time dependence. Amplitude and phase are generally position dependent, however the wave function is a harmonic function of time with the same frequency at all positions.



(a) Figure of wave that combine in phase add up relatively high irradiance (constructive coherent).

(b) Figure of wave that combine π radiance out of phase cancel out and yield zero irradiance (destructive coherent).

Figure 2.1 The figures of coherent waves

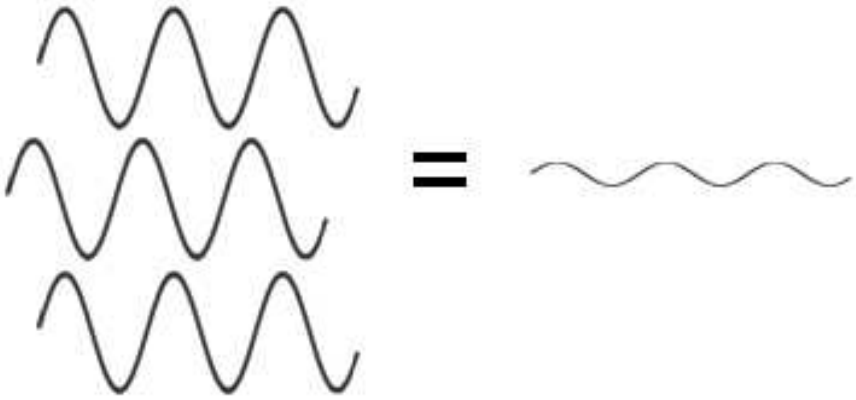


Figure 2.2 The figure of waves that combine with lots of different phases nearly cancel out and yield very low irradiance (incoherent).

2.4 Speckle

Definition 2.9. Speckle is a random pattern which has a negative impact on *coherent imaging*, including ultrasound imaging. It is a result of the superposition of many waves, which have different phases (incoherent).

Speckle occurs in an ultrasound image because the ultrasonic wave encounters rough surfaces that result in the scattering of waves, and we can see in figure 2.3, each scattered wave from a rough surface has a different phase which leads to the forming of speckles.

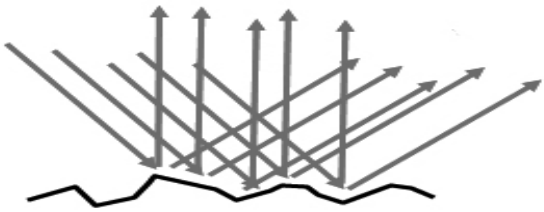


Figure 2.3 Figure of scattering reflection from a rough surface.

Next, we will use the Rayleigh distribution to describe the speckles from the statistical point of view.

A sum of a very large number N of waves which have random phases is considered. Assume that the k-th wave has random amplitude $A_k/\sqrt{N}$ and random phase α_k. The resultant wave a with amplitude $|a|$ and phase α is given by

$$a = |a|e^{i\alpha} = \frac{1}{\sqrt{N}} \sum_{k=1}^{N} A_k e^{i\alpha_k},$$

where $i = \sqrt{-1}$.

Let a_R and a_I denote the real and imaginary parts of the resultant, respectively,

$$\begin{aligned} a_R &= \frac{1}{\sqrt{N}} \sum_{k=1}^{N} A_k \cos\alpha_k, \\ a_I &= \frac{1}{\sqrt{N}} \sum_{k=1}^{N} A_k \sin\alpha_k, \end{aligned}$$

where

$$|a| = \sqrt{a_R^2 + a_I^2}.$$

Goodman (2000) showed that a_R and a_I *are normally distributed*, *have zero mean*, *have the same variance* and *are independent*.

If we consider $|a|$ as a random variable, thus the Rayleigh distribution can be used to describe the speckle statistically and $|a|$ is called a Rayleigh random variable.

Note that the amplitude of the harmonic wave, $|a|$, corresponds to the intensity of the image at each point.

CHAPTER III

CALCULUS OF VARIATIONS AND ROF MODEL

This chapter discusses the calculus of variations which is a mathematical field used for optimization such as the construction of image denoising models. The ROF model, a well-known image denoising model dealing with calculus of variation, is also presented.

3.1 Calculus of Variations

calculus of variations is a field of mathematics that deals with functionals, as opposed to ordinary calculus which deals with functions. Such functionals can be formed as integrals involving an unknown function and its derivatives. The interest is in extremal functions making the functional attain an extremum value. The candidates in the competition for an extremum are functions.

Example 3.1. The problem involves finding the extrema of integrals of the form

$$\mathcal{I} = \iint_{\Omega} F(x, y, u, u_x, u_y) dx dy \tag{3.1}$$

over a bounded region Ω, where F is uniformly continuous on Ω.

Assume that u is the solution, which is continuous, has continuous derivatives up to second order and exists on the boundary of Ω. We will vary u by an arbitrary function $\eta(x, y)$ with $\eta = 0$ on the boundary curve of Ω and define the function u_ϵ by the equation

$$u_\epsilon(x, y) = u(x, y) + \epsilon\eta(x, y),$$

where ϵ is a parameter.

Because of arbitrariness of η, u_ϵ represents any function with continuous second derivatives on Ω. Out of all these u_ϵ, we want to pick the one function that makes $\mathcal{I}$ smallest or largest. Now $\mathcal{I}$ is a function of the parameter ϵ. When $\epsilon = 0$, we have

$$u_\epsilon(x, y) = u(x, y),$$

which is the desired solution. Our problem is to make $\mathcal{I}$ taking its extremum value, when $\epsilon = 0$. In other words, we want

$$\frac{d\mathcal{I}}{d\epsilon}(u + \epsilon\eta)|_{\epsilon=0} = 0.$$

Differentiating equation (3.1) with respect to ϵ, we get

$$\begin{aligned}\frac{d\mathcal{I}}{d\epsilon}(u + \epsilon\eta)|_{\epsilon=0} &= \iint_\Omega \left(F_u\eta + F_{u_x}\eta_x + F_{u_y}\eta_y\right) dxdy \\ &= \iint_\Omega \left(F_u\eta\right) dxdy + \iint_\Omega \left(F_{u_x}\eta_x\right) dxdy + \iint_\Omega \left(F_{u_y}\eta_y\right) dxdy = 0,\end{aligned}$$

which will be transformed by integrating by parts.

Consider $\iint_\Omega \left(F_{u_x}\eta_x\right) dxdy$, we will compute $\int \left(F_{u_x}\eta_x\right) dx$ by integrating by parts. Let $w = F_{u_x}$, we have $dw = \left(\frac{\partial}{\partial x}F_{u_x}\right) dx$, $dv = \left(\eta_x\right) dx$ and $v = \eta$, then

$$\begin{aligned}\int \left(F_{u_x}\eta_x\right) dx &= wv - \int vdw \\ &= F_{u_x}\eta - \int \left(\eta\frac{\partial}{\partial x}F_{u_x}\right) dx.\end{aligned}$$

By Gauss's integral theorem (Courant, 1924), we obtain

$$\iint_\Omega \left(F_{u_x}\eta_x\right) dxdy = \int_\Upsilon \left(F_{u_x}\eta\right) dy - \iint_\Omega \left(\eta\frac{\partial}{\partial x}F_{u_x}\right) dxdy,$$

where Υ is the boundary curve of Ω.

Similarly,

$$\iint_\Omega \left(F_{u_y}\eta_y\right) dxdy = \int_\Upsilon \left(F_{u_y}\eta\right) dx - \iint_\Omega \left(\eta\frac{\partial}{\partial y}F_{u_y}\right) dxdy.$$

Thus, we obtain

$$\begin{aligned}\frac{d\mathcal{I}}{d\epsilon}(u+\epsilon\eta)|_{\epsilon=0} &= \iint_{\Omega}\eta\left(F_u-\frac{\partial}{\partial x}F_{u_x}-\frac{\partial}{\partial y}F_{u_y}\right)dxdy \\ &\quad +\int_{\Upsilon}\eta\left(F_{u_x}\right)dy+\int_{\Upsilon}\eta\left(F_{u_y}\right)dx=0.\end{aligned}$$

Since $\eta = 0$ on the boundary Υ of Ω, the second term and the third term on the right side vanish. Hence

$$\iint_{\Omega}\eta\left(F_u-\frac{\partial}{\partial x}F_{u_x}-\frac{\partial}{\partial y}F_{u_y}\right)dxdy=0.$$

By continuity and arbitrariness of η on Ω, then

$$F_u-\frac{\partial}{\partial x}F_{u_x}-\frac{\partial}{\partial y}F_{u_y}=0.$$

This is equivalent to the equation

$$\frac{\partial}{\partial x}F_{u_x}+\frac{\partial}{\partial y}F_{u_y}-F_u=0, \tag{3.2}$$

which is called Euler-Lagrange differential equation.

There are a lot of works establishing the existence of extrema and characterizing them. In many cases, extremal functions or curves can be expressed as solutions to differential equations. In particular, we will use the Euler-Lagrange differential equation presented in equation (3.2).

3.2 The ROF Model

In image processing, it is important to decrease the noise in the image. If we represent the noisy image as a function $\widetilde{u}$ obtained by adding noise n to a noiseless image u, then $\widetilde{u}$ can be represented by

$$\widetilde{u}(x,y)=u(x,y)+n(x,y), \tag{3.3}$$

where $u(x, y)$ is intensity of desired image at coordinate (x, y), $\widetilde{u}$ is intensity of observed image at coordinate (x, y) and $n(x, y)$ is intensity of additive noise at coordinate (x, y).

Our purpose is to find the desired image u which is the solution of the corresponding denoising problem.

Rudin, Osher and Fatemi (1992) presented a mathematical denoising model called the ROF model which is based on gradient, the least squares problem and calculus of variation. In particular, calculus of variation leads the ROF model to the Euler-Lagrange differential equation similar to example 3.1.

Before discussing the ROF model, we need to review about the gradient and the least square problem.

3.2.1 Gradient

Given a function $f(x, y)$, the partial derivatives f_x and f_y represent the rates of change of f in directions parallel to the x-axes and the y-axes respectively. However, it is also necessary to consider rates of change of $f(x, y)$ in other directions. This is the reason why we study the gradient.

Definition 3.1. Let f be a function of x and y. The **gradient** of f is denoted by ∇f and is defined by

$$\nabla f =< f_x, f_y >$$

and its magnitude is defined by

$$\|\nabla f\| = \sqrt{f_x^2 + f_y^2}.$$

In vector calculus, the gradient is a vector which points in the direction of the greatest rate of increase and whose magnitude is the greatest rate of change. We use the gradient to investigate the directional derivative.

Definition 3.2. Let f be a function of x and y. If $v =< v_1, v_2 >$ is a **unit vector**, then the **directional derivative** of f in the direction of v at (x, y) is denoted by $D_v f(x, y)$ and is defined by

$$D_v f(x, y) = \nabla f(x, y) \cdot v.$$

If θ is the angle between ∇f and v, then

$$\begin{aligned} D_v f &= \nabla f \cdot v \\ &= \|\nabla f\| \|v\| \cos\theta \\ &= \|\nabla f\| \cos\theta. \end{aligned}$$

This equation tells us that the maximum value of $D_v f(x, y)$ is $\|\nabla f\|$ and this maximum occurs when $\theta = 0$, that is when v is in the direction of ∇f. Geometrically, this mean that the surface $z = f(x, y)$ has its *maximum slope* at point (x, y) in the direction of the gradient, where the maximum slope is $\|\nabla f\|$.

3.2.2 The Least Square Problem

A task that occurs in scientific investigation is finding a straight line that fits some set of data points. Typically we have a large number of points (x_i, y_i), where $i = 1, 2, ..., n$, and we have theoretical reason to believe that these points should lie on a straight line. Thus we seek a linear function $p(x) = a + bx$ such that $p(x_i) = y_i$, where $i = 1, 2, ..., n$. In fact, the points will deviate from a straight line, thus it is not possible to find a linear function $p(x)$ that passes through all of them which is the best representation of all data (x_i, y_i). Instead, one settles for a line that fits the points well, in the sense that the errors

$$|y_i - p(x_i)|,$$

where $i = 1, 2, ..., n$ are made as small as possible.

Denote $r =< y_1 - p(x_1), ..., y_n - p(x_n) >$ as the vector of residuals. We can solve our problem by choosing a *vector norm* $\|\cdot\|$.* The solution depends on the choice of norm. If we choose the *Euclidean norm* †, we minimizing the quantity

$$\|r\|_2 = \left(\sum_{i=1}^{n} |y_i - p(x_i)|^2 \right)^{\frac{1}{2}}.$$

To minimize $\|r\|_2$ is equivalent to minimize

$$(\|r\|_2)^2 = \sum_{i=1}^{n} |y_i - p(x_i)|^2.$$

Thus we are minimizing the sum of the squares of the residuals. For this reason the problem of minimizing $\|r\|_2$ is called the *least square problem.*

In the continuous case, the discrete points are replaced by continuous data $\{(x, y(x))|x \in [a, b]\}$. Thus given a function y defined on some bounded interval $[a, b]$, we seek a linear function ψ such that ψ approximates y. As norm $\|\cdot\|$ of a continuous function h on $[a, b]$ we choose

$$\|h\|_2 = \left(\int_a^b |h(x)|^2 dx \right)^{\frac{1}{2}},$$

which is called the L^2-norm. Then the summation in the discrete case is substituted by the integral, and the least square problem in the continuous case is to find a continuous function $\psi(x)$ minimizing

$$\int_a^b |y(x) - \psi(x)|^2 dx.$$

3.2.3 Description of the ROF Model

From the relation between a noisy image $\widetilde{u}$ and a noiseless image u in equation (3.3), we wish to reconstruct u from $\widetilde{u}$. The most conventional method

*See the definition of **vector norm** in Introductory Functional Analysis with Application (Kreyszig, 1988).

†Let $x =< x_1, ..., x_n > \in \mathbb{R}^n$, **Euclidian norm** on $\mathbb{R}^n$ is the vector norm defined by $\|x\| = \left(\sum_{i=1}^{n} |x_i|^2 \right)^{\frac{1}{2}}$.

involves the least squares with the $L^2 - norm$ because this leads to a linear term in the Euler-Lagrange equation.

Rudin et al. (1992) presented the denoising model which applies the solution of the *one-dimensional linear integral equation of the first kind* [‡]. In the two-dimensional case, the problem is to minimize

$$\iint_{\Omega} (u_{xx} + u_{yy})^2 dxdy + \iint_{\Omega} (u - \widetilde{u})^2 dxdy.$$

The first term is a generalization of the one-dimensional case and the second term is the error term. However the result is disappointing in digital image denoising.

After that, they found that when the L^1-norm is applied to the gradient, which is defined by

$$\iint_{\Omega} \|\nabla u\| \, dxdy = \iint_{\Omega} \left(\sqrt{u_x^2 + u_y^2}\right) dxdy,$$

then this L^1 approximation looks better than the L^2 approximation on a computer screen. This is the reason why Rudin et al. use the L^1-norm of the gradient in the ROF model.

Definition 3.3. Let $\widetilde{u}$ be a function describing the noisy image and u a function describing the noiseless image with respect to $\widetilde{u}$. The **ROF model** considers u as a solution to a problem of calculus of variations, which minimizes the functional

$$F(u) = \iint_{\Omega} \left(\sqrt{u_x^2 + u_y^2}\right) dxdy + \lambda \iint_{\Omega} (u - \widetilde{u})^2 dxdy, \tag{3.4}$$

where $\Omega \in \mathbb{R}^2$ is the domain of the image functions and λ is a chosen parameter.

[‡]Let $K(x, y)$ and $g(x)$ be the given bounded functions, the **linear integral equations of the first kind** is written as $\int_a^b K(x, y) f(y) \, dy = g(x)$.

Phillips (1962) showed that finding the solution of this equation is equivalent to minimizing $\int_a^b (f'')^2 ds$.

The first term of equation (3.4) is a regularization term which is the magnitude of ∇u, i.e. it is the maximum rate of change of u. By regularization we mean that the gradients of u over Ω should be small on the average. The second term is the data-fidelity term. In fact, if we minimize this term we can see in equation (3.3) that we find the least square of the noise over the region Ω.

By calculus of variations, the solution of equation (3.4) obtained by the Euler-Lagrange differential equation is satisfied, i.e.

$$\frac{\partial}{\partial x}\left(\frac{u_x}{\sqrt{u_x^2+u_y^2}}\right)+\frac{\partial}{\partial y}\left(\frac{u_y}{\sqrt{u_x^2+u_y^2}}\right)+\lambda(u-\widetilde{u})=0, \tag{3.5}$$

where $\dfrac{\partial u}{\partial N}=0$ on Ω, here N is the normal vector to the boundary Ω.

CHAPTER IV

RESULT AND CONCLUSION

The model for speckle denoising in the ultrasound image is presented in this chapter. Rayleigh distribution are used for the description of the speckle noise occurring in this model. The method of calculus of variation leads the model to the Euler-Lagrange equation. The equation is solved numerically by the gradient descent method. Finally, the experimental results to verify the model and theorems are also presented.

4.1 Description of the Proposed Model

Assume that $\widetilde{u}$ is a given noisy ultrasound image defined on Ω, a bounded open rectangle in $\mathbb{R}^2$ with piecewise *Lipschitz boundary*[*] $\partial\Omega$. We assume that $\widetilde{u}$ is bounded and positive on Ω and $\widetilde{u}_{x,y}$ is the intensity of $\widetilde{u}$ at the location (x, y). Note that $\widetilde{u}$ is assumed to be noiseless on $\partial\Omega$.

Recall that the image intensity of an ultrasound image is a Rayleigh random variable, which has a density function:

$$R_\sigma(r) = \frac{r}{\sigma^2} e^{-\frac{r^2}{2\sigma^2}},$$

where $r \geq 0$ is the image intensity and σ is a parameter.

Let $U_{x,y}$ be a random variable on the set of noiseless images, which corresponds to noiseless image intensity at point (x, y) and $\widetilde{U}_{x,y}$ be a random variable on the set of observed images, which corresponds to the observed image intensity

[*]See the definition of **Lipschitz boundary** in definition 4.5.

at point (x, y). We wish to determine the image u which is most likely given the observed image $\widetilde{u}$.

From the statistical point of view, we are going to find an image u which maximizes the conditional probability that the intensity of a noiseless image is the most likely given the intensity of the observed image for all (x, y). We assume that Ω is pixelleted by $\Omega = \{(x, y)|x, y = 0, \ldots, N-1\}$ and the values of image intensity for each pixel (x, y) are independent, thus the conditional probability mentioned is

$$\prod_{(x,y)\in\Omega} P\left(U_{x,y} = u_{x,y}|\widetilde{U}_{x,y} = \widetilde{u}_{x,y}\right),$$

where $u_{x,y} = u(x, y)$ and $\widetilde{u}_{x,y} = \widetilde{u}$. *Bayes' Rule* says that

$$P\left(U_{x,y} = u_{x,y}|\widetilde{U}_{x,y} = \widetilde{u}_{x,y}\right) = \frac{P\left(\widetilde{U}_{x,y} = \widetilde{u}_{x,y}|U_{x,y} = u_{x,y}\right) P\left(U_{x,y} = u_{x,y}\right)}{P\left(\widetilde{U}_{x,y} = \widetilde{u}_{x,y}\right)},$$

where, at point (x, y), $P\left(U_{x,y} = u_{x,y}|\widetilde{U}_{x,y} = \widetilde{u}_{x,y}\right)$ is the conditional probability of the intensity of the noiseless image u on the condition of the intensity of the observed image $\widetilde{u}$, $P\left(\widetilde{U}_{x,y} = \widetilde{u}_{x,y}|U_{x,y} = u_{x,y}\right)$ is the conditional probability of the intensity of the observed image $\widetilde{u}$ on the condition of the intensity of the noiseless image u, $P(U_{x,y} = u_{x,y})$ is the probability of intensity of the noiseless image and $P\left(\widetilde{U}_{x,y} = \widetilde{u}_{x,y}\right)$ is the probability of intensity of the observed image $\widetilde{u}$.

In order to maximizing $P(U_{x,y} = u_{x,y}|\widetilde{U}_{x,y} = \widetilde{u}_{x,y})$, we are going to find the noiseless image u which maximizes

$$\prod_{(x,y)\in\Omega} P\left(\widetilde{U}_{x,y} = \widetilde{u}_{x,y}|U_{x,y} = u_{x,y}\right) P\left(U_{x,y} = u_{x,y}\right). \tag{4.1}$$

For each (x, y), $\widetilde{u}$ is Rayleigh random variable and its probability density is

$$\begin{aligned} P\left(\widetilde{U}_{x,y} = \widetilde{u}_{x,y}\right) &= R_\sigma(\widetilde{u}_{x,y}) \\ &= \frac{\widetilde{u}_{x,y}}{\sigma^2} e^{-\frac{[\widetilde{u}_{x,y}]^2}{2\sigma^2}}. \end{aligned}$$

Recall that the above density function $R_\sigma(\widetilde{u}_{x,y})$ depends on the parameter σ. Assume the parameter σ of the conditional probability of $\widetilde{u}$ on the condition of the noiseless image u is a function of u, $\sigma = \sigma(u)$. The conditional probability of the intensity of the observed image $\widetilde{u}$ at the point (x, y) is

$$\begin{aligned} P\left(\widetilde{U}_{x,y} = \widetilde{u}_{x,y} | U_{x,y} = u_{x,y}\right) &= R_{\sigma(u_{x,y})}(\widetilde{u}_{x,y}) \\ &= \frac{\widetilde{u}_{x,y}}{\left[\sigma\left(u_{x,y}\right)\right]^2} e^{-\frac{[\widetilde{u}_{x,y}]^2}{2[\sigma(u_{x,y})]^2}}. \end{aligned}$$

Expression (4.1) becomes

$$\left(\prod_{(x,y)\in\Omega} \frac{\widetilde{u}_{x,y}}{\left[\sigma\left(u_{x,y}\right)\right]^2} e^{-\frac{[\widetilde{u}_{x,y}]^2}{2[\sigma(u_{x,y})]^2}} \right) P\left(U_{x,y} = u_{x,y}\right). \tag{4.2}$$

Since the *natural logarithm* function which is denoted by $\ln(x)$ is an increasing continuous function, the function $-\ln(x)$ is a decreasing continuous function. Hence the minimizing of $-\ln\left(\prod_{(x,y)\in\Omega} P\left(\widetilde{U}_{x,y} = \widetilde{u}_{x,y} | U_{x,y} = u_{x,y}\right) P\left(U_{x,y} = u_{x,y}\right) \right)$ is equivalent to the maximizing expression (4.1). Therefore, we seek a minimizer of

$$-\ln\left(\prod_{(x,y)\in\Omega} P\left(\widetilde{U}_{x,y} = \widetilde{u}_{x,y} | U_{x,y} = u_{x,y}\right) \right) - \ln\left(\prod_{(x,y)\in\Omega} P\left(U_{x,y} = u_{x,y}\right) \right). \tag{4.3}$$

The expression (4.3) becomes

$$\sum_{x=0}^{N-1} \sum_{y=0}^{N-1} \left(\frac{[\widetilde{u}_{x,y}]^2}{2[\sigma\left(u_{x,y}\right)]^2} + 2\ln\sigma\left(u_{x,y}\right) - \ln\widetilde{u}_{x,y} \right) - \ln\left(\prod_{(x,y)\in\Omega} P\left(U_{x,y} = u_{x,y}\right) \right).$$

We regard this as a discrete approximation of the functional

$$E(u) = -\ln P(u) + \iint_\Omega \left(\frac{\widetilde{u}^2}{2[\sigma(u)]^2} + 2\ln\sigma(u) - \ln\widetilde{u} \right) dA, \tag{4.4}$$

where $P(u)$ is the probability that the random variable $U_{x,y}$ is equal to the intensity of the noiseless image u at pixel (x, y) for all $(x, y) \in \Omega$. For the model of a variational approach, Green (2002) presents that $P(u)$ is given by

$$P(u) = e^{-\beta \iint_\Omega \left(\sqrt{u_x^2 + u_y^2}\right) dA},$$

where β is a parameter. Hence, functional $E(u)$ becomes

$$E(u) = \beta \iint_{\Omega} \left(\sqrt{u_x^2 + u_y^2} \right) dA + \iint_{\Omega} \left(\frac{\widetilde{u}^2}{2[\sigma(u)]^2} + 2 \ln \sigma(u) - \ln \widetilde{u} \right) dA. \quad (4.5)$$

The Euler-Lagrange equation for minimizing $E(u)$ is

$$\frac{\partial}{\partial x} \left(\frac{u_x}{\sqrt{u_x^2 + u_y^2}} \right) + \frac{\partial}{\partial y} \left(\frac{u_y}{\sqrt{u_x^2 + u_y^2}} \right) + \frac{\sigma'(u)}{\beta[\sigma(u)]^3} \left(\widetilde{u}^2 - 2[\sigma(u)]^2 \right) = 0. \quad (4.6)$$

Since the last term of equation (4.6) is a data-fidelity term (Le, 2005), the constraint vanishing of it where $u = \widetilde{u}$ is considered:

$$\frac{\sigma'(u)}{\beta[\sigma(u)]^3} \left(\widetilde{u}^2 - 2[\sigma(u)]^2 \right) = 0. \quad (4.7)$$

For the sake of the simplicity, function

$$\sigma(u) = \frac{u}{\sqrt{2}},$$

is chosen for satisfying the requirement (4.7). The functional $E(u)$ obtained is

$$E(u) = \beta \iint_{\Omega} \left(\sqrt{u_x^2 + u_y^2} \right) dA + \iint_{\Omega} \left(\frac{\widetilde{u}^2}{u^2} + 2 \ln u - \ln \sqrt{2} - \ln \widetilde{u} \right) dA. \quad (4.8)$$

The functional E is defined on the set of functions u which are of *bounded variation* [†] on Ω such that $\frac{1}{u^2}$ and $\ln u$ belong to $L^1(\Omega)$, i.e. $\iint_{\Omega} \left| \frac{1}{u^2} \right| dA$ and $\iint_{\Omega} |\ln u| \, dA$ exist.

Hence, the requirements which we impose on u are

$$u \in C(\overline{\Omega}), u \in C^2(\Omega) \text{ and } u \text{ is positive on } \Omega. \quad (4.9)$$

For the uniqueness of the solution u, we require that

$$0 < u < \sqrt{3}\widetilde{u}, \quad (4.10)$$

which is explained in section 4.2.

The Euler-Lagrange equation for minimizing $E(u)$ is

$$\frac{\partial}{\partial x} \left(\frac{u_x}{\sqrt{u_x^2 + u_y^2}} \right) + \frac{\partial}{\partial y} \left(\frac{u_y}{\sqrt{u_x^2 + u_y^2}} \right) + \frac{2}{\beta u^3} (\widetilde{u}^2 - u^2) = 0, \quad (4.11)$$

where $u = \widetilde{u}$ on $\partial\Omega$.

[†]See the definition of *bounded variation* in Definition 4.4

4.2 Existence and Uniqueness

Next, we will show existence and uniqueness of the minimizer for model (4.8).

In order to show the existence of the minimizer of our model, the *compactness-like of L^1 in the space of function of bounded variation* has to be claimed. *Sobolev space* and *space of bounded variation* are presented to satisfy the claim.

Definition 4.1. Let Ω be a subset of $\mathbb{R}^n$. A function f belongs to **Sobolev space** $W^{1,p}(\Omega)$ if $f \in L^p(\Omega)$, i.e. $\|f\|_{L^p}$ is finite and all weak partial derivatives $\dfrac{\partial f}{\partial x_i}$ exist and belong to $L^p(\Omega)$, $i = 1, 2, ..., n$.

Here the norm of $L^p(\Omega)$ is defined by

$$\|f\|_{L^p} = \left(\int_\Omega |f|^p \right)^{\frac{1}{p}}$$

and the norm of $W^{1,p}(\Omega)$ is defined by

$$\|f\|_{W^{1,p}(\Omega)} = \left(\int_\Omega \|f\|^p + |\nabla f|^p \right)^{\frac{1}{p}}.$$

Definition 4.2. Let $f : \mathbb{R}^n \to \mathbb{R}$.

i) The **support** of f is the closure of the set of points where f is nonzero, i.e.

$$\text{spt} f = \overline{\{x \in \mathbb{R}^n, f(x) \neq 0\}},$$

where $\overline{\{.\}}$ is the closure of the set.

ii) The function f is said to have **compact support** if spt$f$ is a compact set.

Definition 4.3. $C^k(\Omega)$ is the set of functions f defined on Ω whose k-order derivatives exist and are continuous.

The set of functions f which belong to $C^k(\Omega)$ for all $k \in \mathbb{N}$ is denoted by $C^\infty(\Omega)$.

Also, set

$$C_c^1(\Omega) = \{f \in C(\Omega) : f \text{ has compact support}\}.$$

Definition 4.4. Let Ω be an open bounded subset of $\mathbb{R}^n$. A function $f \in L^1(\Omega)$ is said to be of **bounded variation** in Ω, if

$$\|Df\|(\Omega) = \sup\{\int_\Omega f \mathrm{div}\varphi|\ \varphi \in C_c^1(\Omega, \mathbb{R}^n), \|\varphi(x)\| \leq 1, \forall x \in \Omega\} < \infty.$$

Here $C_c^1(\Omega, \mathbb{R}^n)$ denotes the set of $\varphi : \Omega \to \mathbb{R}^n$ which is continuously differentiable vector function and its compact support is contained in Ω. We set

$$BV(\Omega) = \{f \in L^1(\Omega) : \|Df\|(\Omega) < \infty\}.$$

The norm on $BV(\Omega)$ is defined by

$$\|f\|_{BV(\Omega)} \equiv \|Df\|(\Omega) + \|f\|_{L^1(\Omega)}.$$

$BV(\Omega)$ becomes a Banach space. $\|Df\|(\Omega)$ is called the **total variation of f on Ω**.

Remark If $f \in C^1(\Omega)$ and f and its first-order partial derivatives lie in $L^1(\Omega)$, then

$$\|Df\|(\Omega) = \int_\Omega \|\nabla f\|.$$

Theorem 4.1. *Let $\{f_k\} \subset BV(\Omega)$ and suppose that $f_k \to f$ in the norm of $L^1(\Omega)$. Then*

1. *$f \in BV(\Omega)$.*
2. *$\|Df\|(\Omega) \leq \lim_{k\to\infty} \inf \|Df_k\|(\Omega)$.*

See proof of the theorem in Evans (1992).

Definition 4.5. Let Ω be an open bounded subset of $\mathbb{R}^n$. We say that Ω is a bounded open set with **Lipschitz boundary** if for every $a \in \partial\Omega$ there exist a neighborhood $U \in \mathbb{R}^n$ of a and a bijective map $H : \overline{Q} \to \overline{U}$, where

$$\begin{aligned} Q &= \{a = (a_1, ..., a_n) \in \mathbb{R}^n, |a_j| < 1, j = 1, 2, ..., n\}, \\ H &\in C(\overline{Q}), \\ H^{-1} &\in C(\overline{U}), \\ H(Q_+) &= U \cap \Omega, \\ H(Q_0) &= U \cap \partial\Omega \\ H &\in C^{0,1}(\overline{Q}), \end{aligned}$$

where $Q_+ = \{a \in Q, a_n > 0\}$, $Q_0 = \{a \in Q, a_n = 0\}$ and $C^{0,1}(\overline{Q})$ is the set of $f \in C(\overline{Q})$ so that

$$\sup_{\substack{x,y \in K \\ x \neq y}} \left\{ \frac{|f(x) - f(y)|}{\|x - y\|} \right\} < \infty,$$

for every compact set $K \subset \overline{Q}$.

Theorem 4.2. *Let Ω be an open bounded subset of $\mathbb{R}^n$ with Lipschitz boundary. Assume $\{f_k\}$ is a sequence in $BV(\Omega)$ satisfying*

$$\|f_k\|_{BV(\Omega)} \leq M, \forall k.$$

Then, there exist a subsequence $\{f_{k_j}\}$ and a function $f \in BV(\Omega)$ such that

$$f_{k_j} \to f$$

in the norm of $L^1(\Omega)$.

See proof of the theorem in Evans (1992).

Remark This theorem says that subsets of $BV(\Omega)$ which are bounded under $\|\cdot\|_{BV(\Omega)}$ are even compact under the norm of $L^1(\Omega)$.

Additionally, for the uniqueness of the minimizer of the denoising model, convexity is considered.

Definition 4.6. A subset M of a vector space X is said to be **convex** if $y, z \in M$ implies that the line segment

$$L = \{v = \alpha y + (1-\alpha)z | 0 \leq \alpha \leq 1\}$$

is a subset of M.

Definition 4.7. A functional F is said to be **convex** if its domain $\mathbb{D}(F)$ is a convex set and for every $a, b \in \mathbb{D}(F)$,

$$F(\lambda a + (1-\lambda)b) \leq \lambda F(a) + (1-\lambda)F(b),$$

where $0 \leq \lambda \leq 1$. In additional if for every $a, b \in \mathbb{D}(F)$, $a \neq b$,

$$F(\lambda a + (1-\lambda)b) < \lambda F(a) + (1-\lambda)F(b),$$

where $0 < \lambda < 1$, then F is said to be a **strictly convex**.

Theorem 4.3. *If F in equation* (3.1) *is strictly convex and the minimizer of the equation* (3.1) *exists, then the minimizer of* (3.1) *is unique.*

Proof. Assume that u and v are two minimizers of equation (3.1) such that $u \neq v$, m denoting the value of the minimizer. Define

$$w = \frac{1}{2}u + \frac{1}{2}v.$$

So $w_x = \frac{1}{2}u_x + \frac{1}{2}v_x$ and $w_y = \frac{1}{2}u_y + \frac{1}{2}v_y$.

By strict convexity of F we obtain

$$\begin{aligned} \frac{1}{2}F(x,y,u,u_x,u_y) + \frac{1}{2}F(x,y,v,v_x,v_y) &> F\left(x, y, \frac{1}{2}u + \frac{1}{2}v, \frac{1}{2}u_x + \frac{1}{2}v_x, \frac{1}{2}u_y + \frac{1}{2}v_y\right) \\ &= F(x,y,w,w_x,w_y) \end{aligned}$$

and then

$$m = \frac{1}{2}\mathcal{I}(u) + \frac{1}{2}\mathcal{I}(v) > \mathcal{I}(w) \geq m.$$

This is a contradiction. Hence, our assumption is false. Because of the arbitrariness of u and v, we conclude that if the minimizer of the equation (3.1) exists, it is unique. □

Lemma 4.4. *If $F : (a, b) \to \mathbb{R}$ is continuously twice differentiable and $F''(u) > 0$, for every $u \in (a, b)$ then, F is strictly convex.*

Proof. The *Taylor series expansion* of F about the point $u_0 \in (a, b)$ is

$$F(u) = F(u_0) + F'(u_0)(u - u_0) + \frac{1}{2}F''(\overline{u})(u - u_0)^2,$$

where $\min(u_0, u) < \overline{u} < \max(u_0, u)$.

If $F''(u) > 0$, for every $u \neq u_0$ then the last term is positive.

Let $u_0 = \lambda u_1 + (1 - \lambda)u_2$ where $0 < \lambda < 1$. Then

$$F(u) > F(u_0) + F'(u_0)(u - (\lambda u_1 + (1 - \lambda)u_2)).$$

For the case $u = u_1$,

$$F(u_1) > F(u_0) + F'(u_0)(1 - \lambda)(u_1 - u_2).$$

This implies that

$$\lambda F(u_1) > \lambda F(u_0) + \lambda(1 - \lambda)F'(u_0)(u_1 - u_2).$$

In the case $u = u_2$,

$$F(u_2) > F(u_0) + F'(u_0)(\lambda)(u_2 - u_1).$$

This implies that

$$(1 - \lambda)F(u_2) > (1 - \lambda)F(u_0) - \lambda(1 - \lambda)F'(u_0)(u_1 - u_2).$$

Combine the inequalities, we obtain

$$\lambda F(u_1) + (1-\lambda)F(u_2) > F(u_0) = F(\lambda u_1 + (1-\lambda)u_2)$$

and get the strictly convexity result for arbitrary u_1, u_2 such that $u_1 \neq u_2$. □

Lemma 4.5. *Let Ω be an open bounded subset of $\mathbb{R}^2$, $\widetilde{u}$ be a continuous positive bounded function on Ω and*

$$\widehat{W} = \left\{u : \overline{\Omega} \to \mathbb{R} | u \text{ satisfies expression (4.9) and inequality (4.10)}\right\}$$

Let $\widehat{J} : \widehat{W} \to C(\overline{\Omega})$ be defined by

$$\widehat{J}(u) = \frac{\widetilde{u}^2}{u^2} + 2\ln u + \mathcal{F}(\widetilde{u}),$$

$\mathcal{F}(\widetilde{u})$ being a constant depending on $\widetilde{u}$. Then, $\widehat{J}(u)$ is strictly convex on $\widehat{W}$.

Proof. One easily verifies that $\widehat{W}$ is convex. Next for fixed constants $c > 0$ and c_1, consider the function $F : (0, \sqrt{3c}) \to \mathbb{R}$ given by

$$F(u) = \frac{c}{u^2} + 2\ln u + c_1.$$

Since $F''(u) = 2\left(\dfrac{3c - u^2}{u^4}\right) > 0, \forall u \in (0, \sqrt{3c})$, it follows from lemma 4.4 that F is strictly convex on $(0, \sqrt{3c})$. That is,

$$F(\lambda u + (1-\lambda)v) < \lambda F(u) + (1-\lambda)F(v), \tag{4.12}$$

$\forall u, v \in (0, \sqrt{3c})$ and $0 < \lambda < 1$. It follows from inequality (4.12) that for each $w \in \Omega$, $c = \widetilde{u}^2(w)$ and $c_1 = \mathcal{F}(\widetilde{u}(w))$, $\forall u, v \in \widehat{W}$ and $0 < \lambda < 1$,

$$\widehat{J}(\lambda u(w) + (1-\lambda)v(w)) < \lambda \widehat{J}(u(w)) + (1-\lambda)\widehat{J}(v(w)),$$

which proves the lemma. □

Remark For the functional

$$J(u) = \iint_{\Omega} \left(\frac{\widetilde{u}^2}{u^2} + 2\ln u + \mathcal{F}(\widetilde{u}) \right) dA, \tag{4.13}$$

if $J(u)$ has a minimizer then theorem 4.3 and lemma 4.5 say $J(u)$ must has a unique minimizer.

Theorem 4.6. *Let Ω be an open bounded subset of $\mathbb{R}^2$ with Lipschitz boundary.Given $\widetilde{u} \in BV(\Omega)$ satisfying $0 < m \leq \widetilde{u}(x,y) \leq M$, almost everywhere $(x,y) \in \Omega$, fix s, $1 < s < \sqrt{3}$,*

$$W = \{u \in BV(\Omega) : 0 < m \leq u(x,y) \leq s\widetilde{u}(x,y), \text{ almost everywhere } (x,y) \in \Omega\}.$$

Let $E : W \to \mathbb{R}$ be given by

$$E(u) = \|Du\|(\Omega) + J(u),$$

where $J(u)$ is defined as equation (4.13). Then E has a unique minimizer.

Proof. **1. Prove the existence of the minimizer**.

Note first that by choice of u, $E(u)$ is defined for all $u \in W$. In fact we have

$$\begin{aligned} m_0 &:= \iint_{\Omega} \left(\frac{m^2}{3M^2} + 2\ln m + \mathcal{F}(\widetilde{u}) \right) dA \\ &\leq \iint_{\Omega} \left(\frac{\widetilde{u}^2}{u^2} + 2\ln u + \mathcal{F}(\widetilde{u}) \right) dA \\ &\leq \iint_{\Omega} \left(\frac{M^2}{m^2} + 2\ln M + \mathcal{F}(\widetilde{u}) \right) dA \ =: \ M_0. \end{aligned} \tag{4.14}$$

In particular, $J(u)$ is bounded below. Since $\|Du\|(\Omega) \geq 0$, then the functional $E(u)$ is bounded below. Thus there exists a sequence $\{u_n\}$ in W minimizing E, that is

$$E(u_n) \to b := \inf\{E(u) : u \in W\}.$$

We need to show that there exists $u_0 \in W$ such that $E(u_0) = b$.

Now as u_n minimizes E, the sequence $\{E(u_n)\}$ is bounded, hence the sequence $\{\|Du_n\|(\Omega)\}$ is bounded. Also, $\{\|u_n\|_{L^1(\Omega)}\}$ is bounded, in fact,

$$m|\Omega| \leq \|u\|_{L^1(\Omega)} \leq M|\Omega|, \forall u \in W,$$

where $|\Omega|$ is an area of Ω. Hence, $\{u_n\}$ is a bounded sequence in the norm of $BV(\Omega)$. Thus by theorem 4.2, there exist $u_0 \in BV(\Omega)$ and a subsequence $\{u_{n_k}\}$ such that $\{u_{n_k}\} \to u_0$ in the norm $\|\cdot\|_{L^1(\Omega)}$.

Since every convergent sequence in $L^1(\Omega)$ possesses a subsequence *converging pointwise almost everywhere*, we may assume, replacing $\{u_{n_k}\}$ by a suitable subsequence, that

$$u_{n_k}(x,y) \to u_0(x,y), \text{ almost everywhere } \Omega.$$

In particular,

$$0 < m \leq u_0(x,y) \leq s\widetilde{u}(x,y), \text{ almost everywhere } \Omega$$

and hence $u_0 \in W$.

Now by theorem 4.1, and as $\{u_{n_k}\}$ is bounded in $BV(\Omega)$,

$$\|Du_0\|(\Omega) \leq \lim_{k\to\infty} \|Du_{n_k}\|(\Omega). \tag{4.15}$$

On the other hand, by expression (4.14) we can apply the *Dominated Convergence Theorem* to obtain that

$$\begin{aligned} J(u_0) &= \iint_\Omega \lim_{k\to\infty} \left(\frac{\widetilde{u}^2}{u_{n_k}^2} + 2\ln u_{n_k} + \mathcal{F}(\widetilde{u}) \right) dA \\ &= \lim_{k\to\infty} \iint_\Omega \left(\frac{\widetilde{u}^2}{u_{n_k}^2} + 2\ln u_{n_k} + \mathcal{F}(\widetilde{u}) \right) dA \\ &= \lim_{k\to\infty} J(u_{n_k}). \end{aligned} \tag{4.16}$$

Combining expression (4.15) and (4.16) then

$$\begin{aligned} E(u_0) &= J(u_0) + \|Du_0\|(\Omega) \\ &\leq \lim_{k\to\infty} J(u_{n_k}) + \lim_{k\to\infty} \|Du_{n_k}\|(\Omega) \\ &= \lim_{k\to\infty} E(u_{n_k}) \;=\; b \end{aligned}$$

since the sequence $\{u_n\}$ minimizes E. This proves existence of a minimizer u_0.

2. Prove the uniqueness of the minimizer.

Observe that W is a convex set. By convexity of $\|\nabla u\|$ and by lemma 4.5, it implies uniqueness of the minimizer of $E(u)$. □

4.3 Numerical Scheme

Consider the problem

$$u_t = \frac{\partial}{\partial x}\left(\frac{u_x}{\sqrt{u_x^2+u_y^2}}\right) + \frac{\partial}{\partial y}\left(\frac{u_y}{\sqrt{u_x^2+u_y^2}}\right) + \frac{2}{\beta u^3}(\widetilde{u}^2 - u^2), \tag{4.17}$$

where $u(x,y,0)$ is given and $u = \widetilde{u}$ on the boundary $\partial\Omega$ of Ω and Ω is a unit rectangle. Here $u = u(x,y,t)$ is a dependent variable, x, y, t are independent variables and $\widetilde{u}(x,y)$ is a given function of spatial variables x, y. In order to solve problem (4.17) numerically, the spatial space of domain is considered as a square grid with N points width and N points height. The grid point (i,j) corresponds to location (x_i, y_j), $i = 0 \ldots N-1, j = 0 \ldots N-1$, where $x_i = ih$, $y_j = jh$ and $Nh = 1$.

Denote $u_{ij}^n = u(x_i, y_j, t_n)$ where $t_n = n\Delta t$, $n = 0, 1, 2, ...$ and Δt is step size. Let $u_{ij}^0 = \widetilde{u}_{ij}$, Rudin (1992) shows that the numerical scheme of problem (4.17) is

$$\begin{aligned} u_{ij}^{n+1} &= u_{ij}^n + \frac{\Delta t}{h}\left[\Delta_-^x\left(\frac{\Delta_+^x u_{ij}^n}{((\Delta_+^x u_{ij}^n)^2 + (m(\Delta_+^y u_{ij}^n, \Delta_-^y u_{ij}^n))^2)^{1/2}}\right)\right] \\ &\quad + \frac{\Delta t}{h}\left[\Delta_-^y\left(\frac{\Delta_+^y u_{ij}^n}{((\Delta_+^y u_{ij}^n)^2 + (m(\Delta_+^x u_{ij}^n, \Delta_-^x u_{ij}^n))^2)^{1/2}}\right)\right] \\ &\quad + \Delta t\left[\frac{2}{\beta(u_{ij}^n)^3}((\widetilde{u}_{ij})^2 - (u_{ij}^n)^2)\right], \end{aligned} \tag{4.18}$$

with boundary conditions

$$\begin{aligned} u_{0j}^n &= \widetilde{u}_{0j} \\ u_{(N-1)j}^n &= \widetilde{u}_{(N-1)j} \\ u_{i0}^n &= \widetilde{u}_{i0} \\ u_{i(N-1)}^n &= \widetilde{u}_{i(N-1)} \end{aligned}$$

where $\Delta_{\pm}^x \Theta_{ij} = \pm(\Theta_{(i\pm1)j} - \Theta_{ij})$ and similarly for $\Delta_{\pm}^y \Theta_{ij}$, the step size Δt and h are chosen for stability such that

$$\frac{\Delta t}{h} \leq 1,$$

$$m(a,b) = (\frac{\text{sgn}(a) + \text{sgn}(b)}{2})\min(|a|, |b|)$$

and

$$\text{sgn}(x) = \begin{cases} -1 & \text{if } x < 0 \\ 0 & \text{if } x = 0 \\ 1 & \text{if } x > 0 \end{cases} .$$

Note that if u_{ij}^n converge as $n \to \infty$, then $\dfrac{u_{ij}^{n+1} - u_{ij}^n}{\Delta t} \to 0$ as $n \to \infty$. Thus, the numerical solution of problem (4.18) will converge to the approximated solution of equation

$$\frac{\partial}{\partial x}\left(\frac{u_x}{\sqrt{u_x^2 + u_y^2}}\right) + \frac{\partial}{\partial y}\left(\frac{u_y}{\sqrt{u_x^2 + u_y^2}}\right) + \frac{2}{\beta u^3}(\widetilde{u}^2 - u^2) = 0,$$

where $u = \widetilde{u}$ on $\partial\Omega$, which is the noiseless image of our model.

4.4 Numerical Results

To verify the theoretical part, we use some images in our experiments. The correlation coefficients of the original images and the noisy images are compared with the correlation coefficients of the original images and the reconstructed images.

First, speckle noise with 0.02 variance is added in the original pattern image by MATLAB software version 7.2. Correlation coefficients of the original image and the noisy image is 0.9678 while correlation coefficients of the original image and reconstructed images with respective to the number of iterative loops are shown in table 4.1. They are higher than 0.9678.

Table 4.1 Correlation coefficients of reconstructed pattern images

Iterative loops	ROF Model	Model by Le et al.	Proposed Model
0	0.9678	0.9678	0.9678
200	0.9882	0.9960	0.9963
250	0.9889	0.9971	0.9974
300	0.9893	0.9978	0.9980
350	0.9895	0.9981	0.9982

Furthermore, we use the Lenna image which is a well-known image in the field of image processing in our experiment. Speckle noise with 0.02 variance is added in the original image by MATLAB software. Similarly, correlation coefficients are compared and they are shown in table 4.2. The correlation coefficient of the original image and noisy image is 0.9444 while the correlation coefficients of the original image and reconstructed images are all higher.

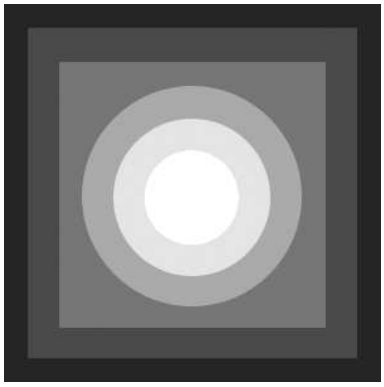
We found that after enhancing the images by the numerical process, the correlation coefficient of the original image and reconstructed images are closer to 1 than the correlation coefficient of the original image and noisy images. This shows that the original image and the reconstructed images have better relationship and our result is claimed. The results show that the noise can be removed by the numerical process.

Table 4.2 Correlation coefficients of reconstructed Lenna images.

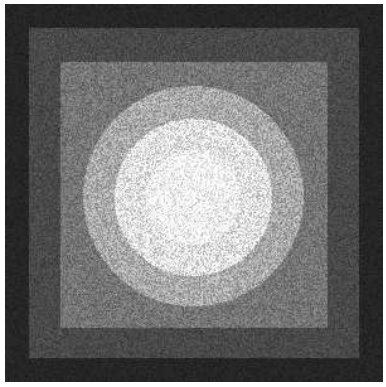
Iterative loops	ROF Model	Model by Le et al.	Proposed Model
0	0.9444	0.9444	0.9444
80	0.9663	0.9725	0.9730
120	0.9704	0.9798	0.9804
160	0.9728	0.9843	0.9848
200	0.9743	0.9868	0.9871

Additionally, if the correlation coefficients of the reconstructed images is used to compare the results of models, the proposed model provides better results than the results of ROF model and the model by Le et al.

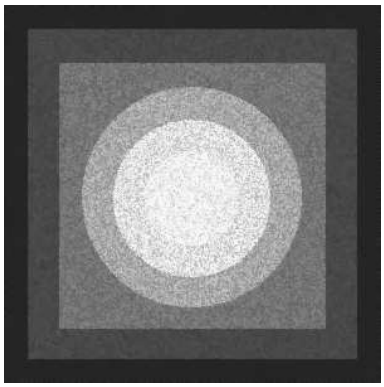
The output of the prototype software shows that after enhancing the ultrasound image, one obtain a smoother image as presented in figure 4.9(a) and figure 4.9(b) which is 100-loops iterative process reconstructed ultrasound image.



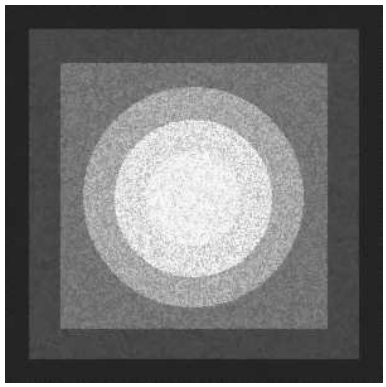
(a) Original pattern image.



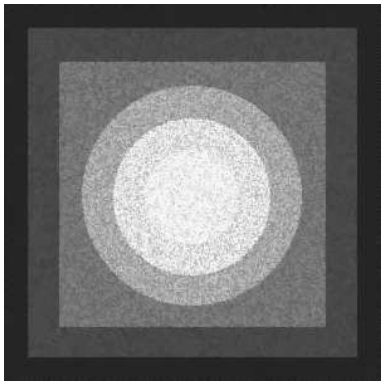
(b) Speckle noisy pattern image.



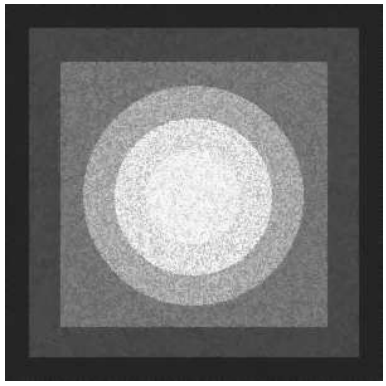
(c) 200-loops iterative process reconstructed image.



(d) 250-loops iterative process reconstructed image.

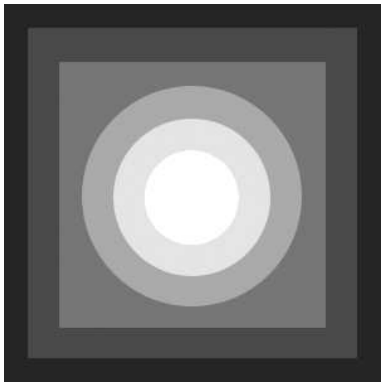


(e) 300-loops iterative process reconstructed image.

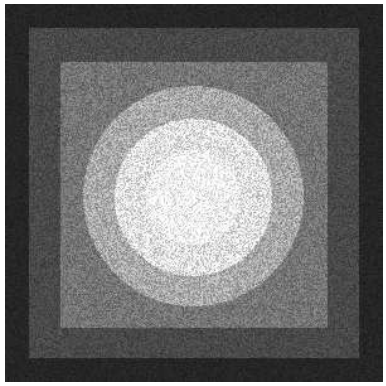


(f) 350-loops iterative process reconstructed image.

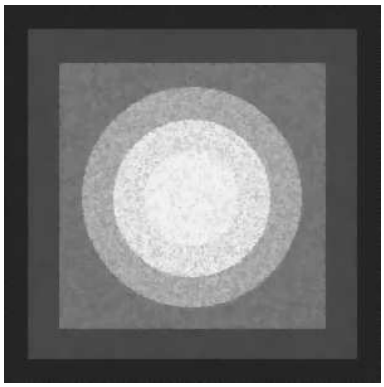
Figure 4.1 The figures of pattern images reconstructed by ROF model.



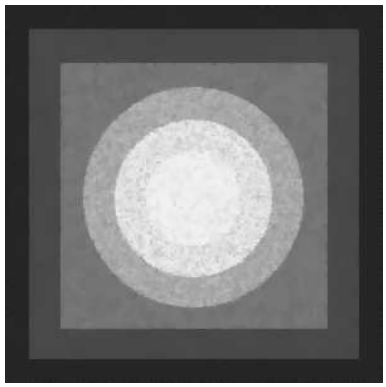
(a) Original pattern image.



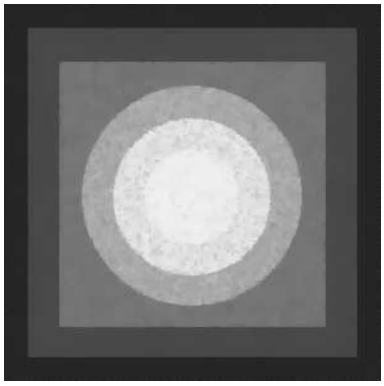
(b) Speckle noisy pattern image.



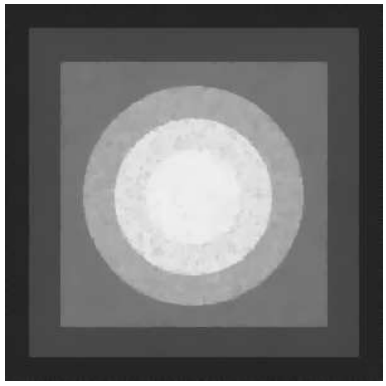
(c) 200-loops iterative process reconstructed image.



(d) 250-loops iterative process reconstructed image.

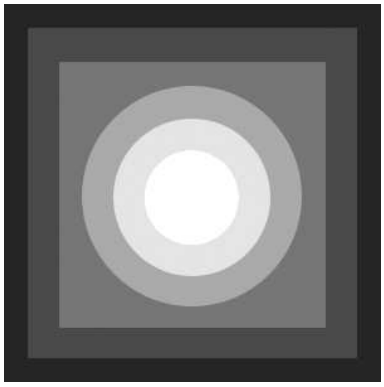


(e) 300-loops iterative process reconstructed image.

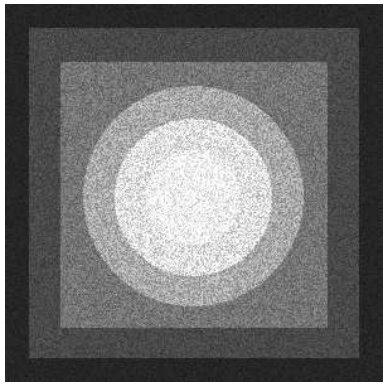


(f) 350-loops iterative process reconstructed image.

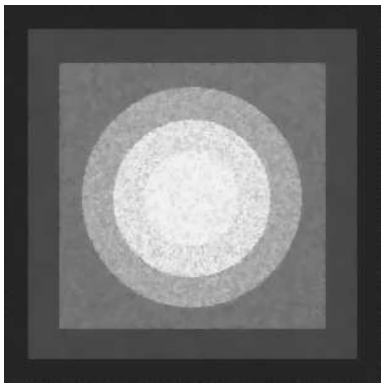
Figure 4.2 The figures of pattern images reconstructed by Le et al.'s model



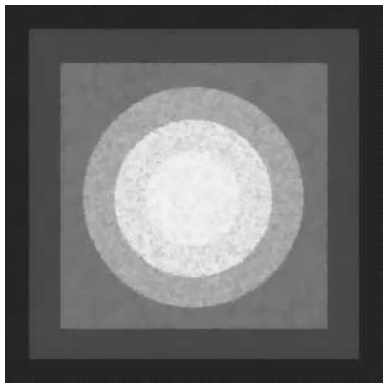
(a) Original pattern image.



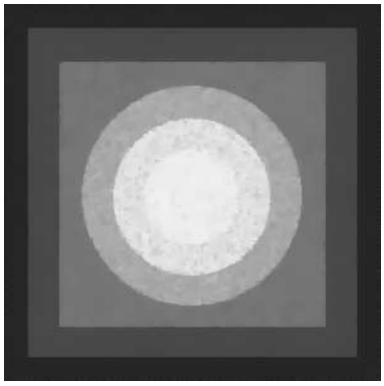
(b) Speckle noisy pattern image.



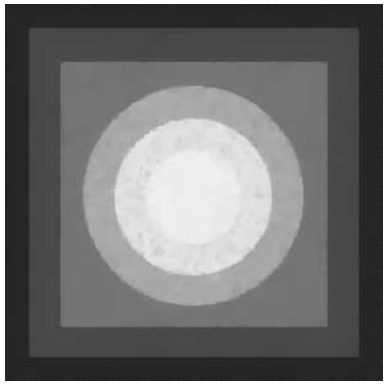
(c) 200-loops iterative process reconstructed image.



(d) 250-loops iterative process reconstructed image.



(e) 300-loops iterative process reconstructed image.



(f) 350-loops iterative process reconstructed image.

Figure 4.3 The figures of pattern images reconstructed by Proposed model.



(a) Original Lenna image.



(b) Speckle noisy Lenna image.



(c) 80-loops iterative process reconstructed image.



(d) 120-loops iterative process reconstructed image.



(e) 160-loops iterative process reconstructed image.



(f) 200-loops iterative process reconstructed image.

Figure 4.4 The figures of Lenna images reconstructed by ROF model.



(a) Original Lenna image.



(b) Speckle noisy Lenna image.



(c) 80-loops iterative process reconstructed image.



(d) 120-loops iterative process reconstructed image.



(e) 160-loops iterative process reconstructed image.



(f) 200-loops iterative process reconstructed image.

Figure 4.5 The figures of Lenna images reconstructed by Le et al.'s model.



(a) Original Lenna image.



(b) Speckle noisy Lenna image.



(c) 80-loops iterative process reconstructed image.



(d) 120-loops iterative process reconstructed image.

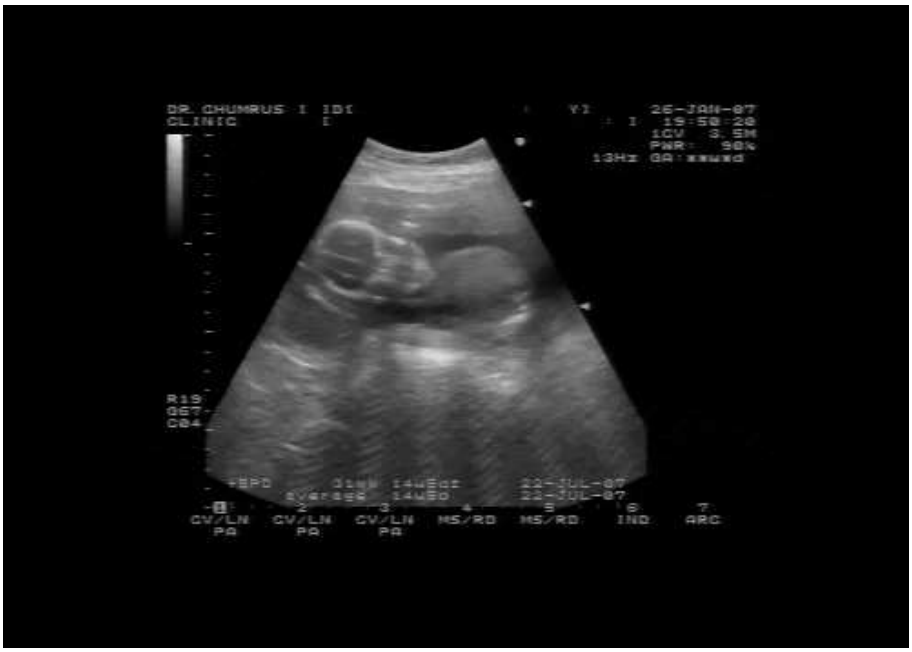


(e) 160-loops iterative process reconstructed image.

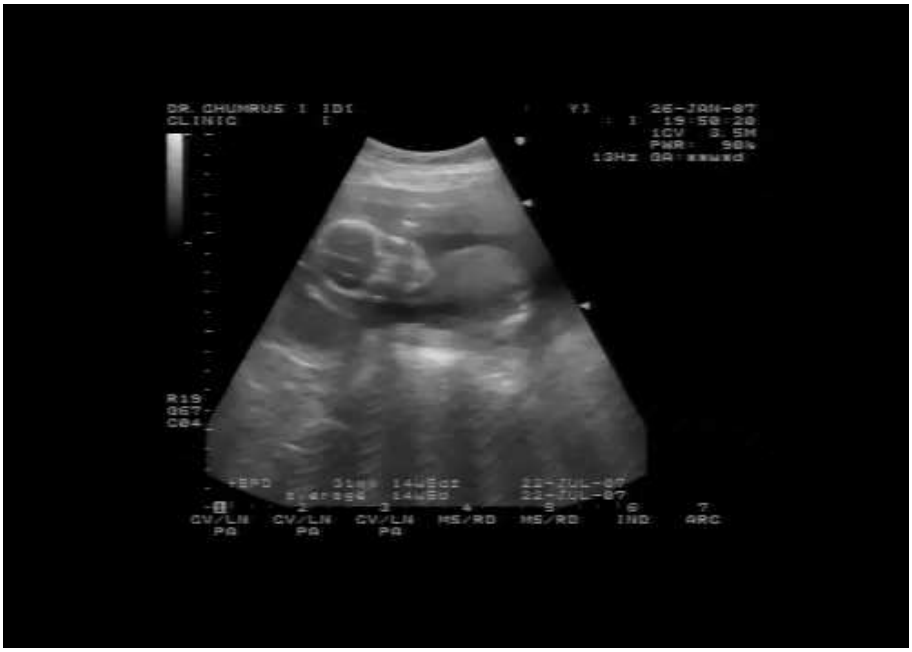


(f) 200-loops iterative process reconstructed image.

Figure 4.6 The figures of Lenna images reconstructed by proposed model.

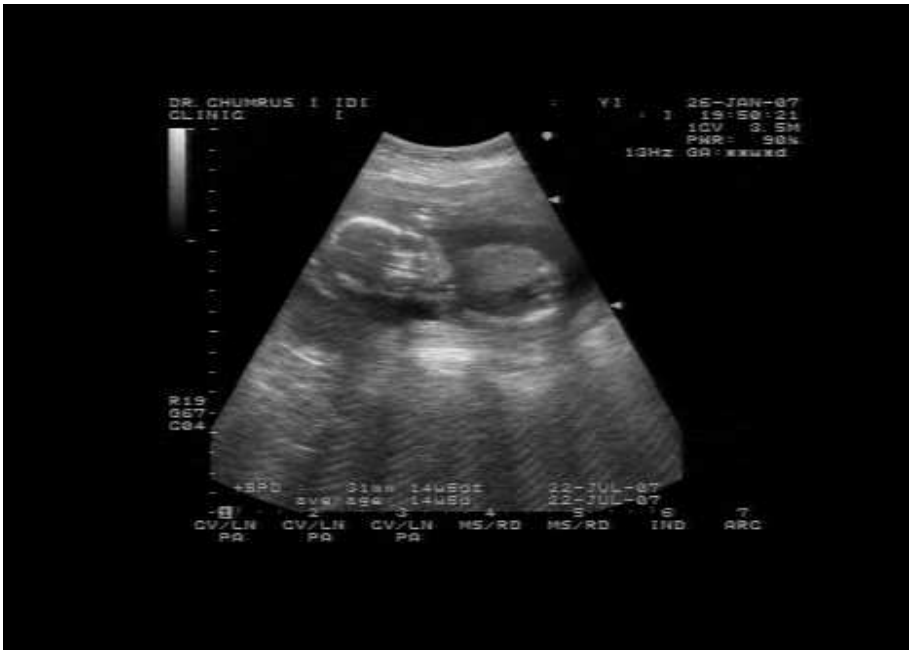


(a) Original ultrasound image (Provided by Dr.Chumrus Sakulpaisarn).

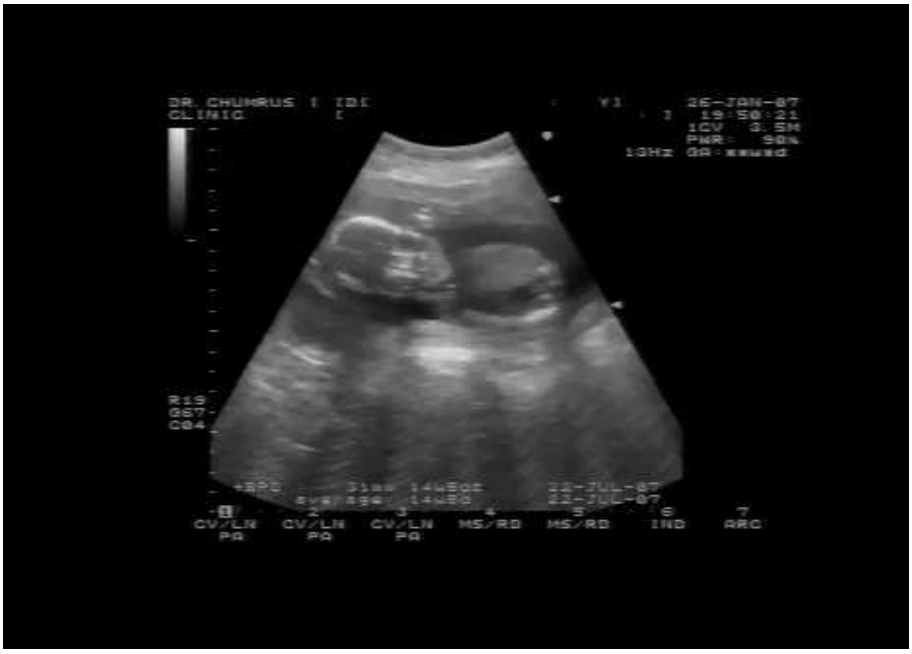


(b) 100-loops iterative process reconstructed ultrasound image.

Figure 4.7 The figures of ultrasound images reconstructed by ROF model.

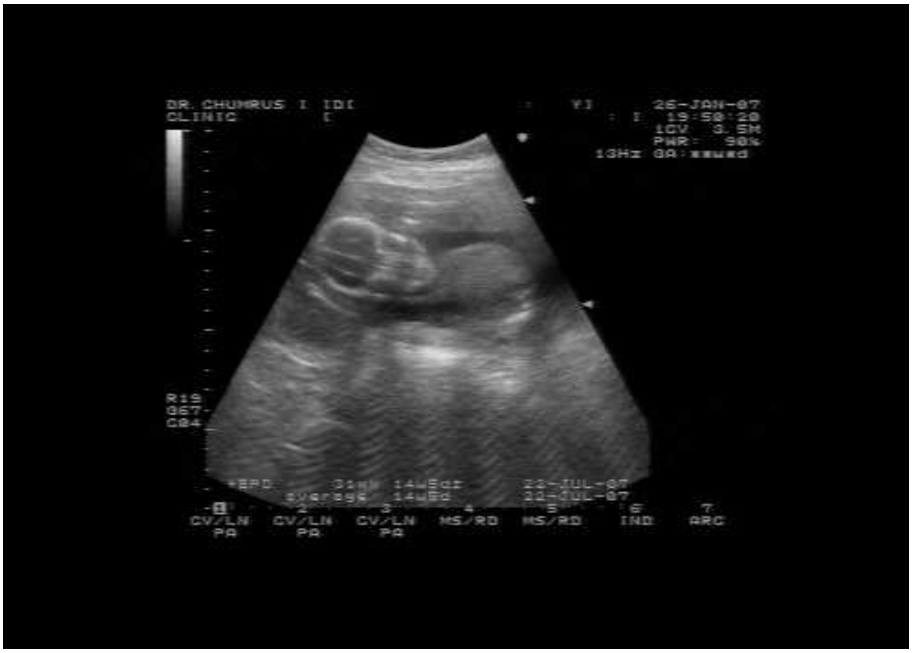


(a) Original ultrasound image (Provided by Dr.Chumrus Sakulpaisarn).

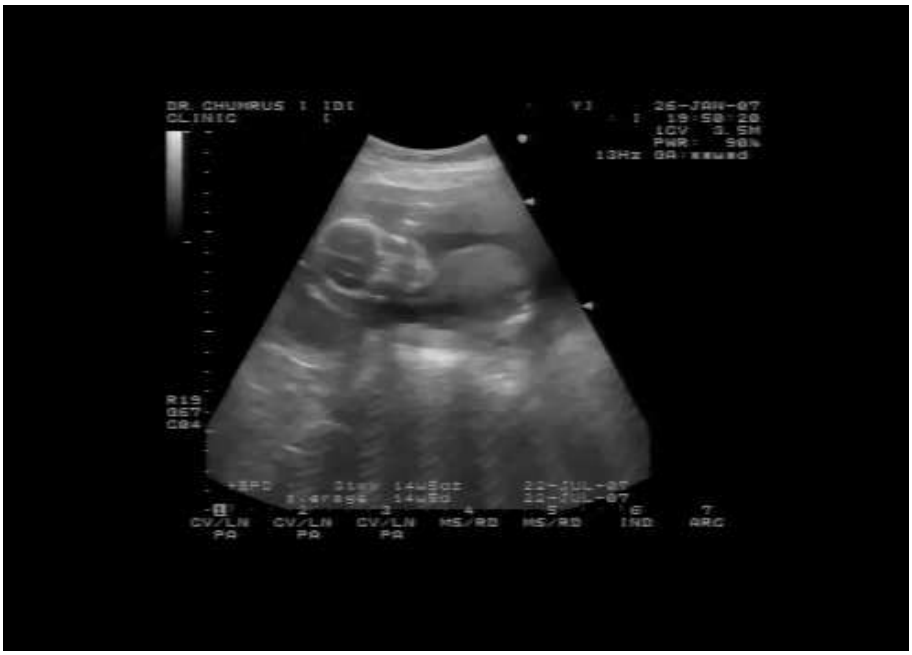


(b) 100-loops iterative process reconstructed ultrasound image.

Figure 4.8 The figures of ultrasound images reconstructed by Le et al.'s model.



(a) Original ultrasound image (Provided by Dr.Chumrus Sakulpaisarn).



(b) 100-loops iterative process reconstructed ultrasound image.

Figure 4.9 The figures of ultrasound images reconstructed by proposed model.

4.5 Conclusion

A new model for speckle reduction of ultrasound images is presented. The model is minimizing the functional

$$E(u) = \beta \iint_{\Omega} \left(\sqrt{u_x^2 + u_y^2} \right) dA + \iint_{\Omega} \left(\frac{\widetilde{u}^2}{u^2} + 2 \ln u + \mathcal{F}(\widetilde{u}) \right) dA,$$

where β is a chosen parameter and $\mathcal{F}(\widetilde{u})$ is a function of $\widetilde{u}$. The model is based on calculus of variations which leads to the Euler-Lagrange differential equation:

$$\frac{\partial}{\partial x} \left(\frac{u_x}{\sqrt{u_x^2 + u_y^2}} \right) + \frac{\partial}{\partial y} \left(\frac{u_y}{\sqrt{u_x^2 + u_y^2}} \right) + \frac{2}{\beta u^3} (\widetilde{u}^2 - u^2) = 0,$$

where $u = \widetilde{u}$ on $\partial\Omega$ and approximation of the solution is by gradient descent method. Our technique can reduce the noise better than the ROF model. However, the result of the reconstructed images by our model are almost identical to the one by Le. The constraint is the processing time required. Moreover, because we work with the gray scale 256 bits mode, errors may arise from the rounding function in the software implementation.

REFERENCES

REFERENCES

Anaesthesia UK. **Types of ultrasound** [On-line]. Available: http://www.frca.co.uk/SectionContents.aspx?sectionid=86.

Anton H., Bivens I. and Davis S. (2002) **Calculus**, JOHN WILEY & SONS.

Aubert G. and Aujol J.F. (2008), **A variatioanal Approach to Remove Multiplicative Noise.**, SIAM Journal on Applied Mathematics.

Courant R. and Hilbert D. (1989) **Methods of Mathematical Physics**, JOHN WILEY & SONS.

Cullen C.G. (1994) **An Introduction to Numerical Linear Algebra**, International Thomson Publishing.

Dacorogna B. (2004) **Introduction to the Calculus of Variations**, Imperial College Press.

Evans L.C. and Garicpy R.F. (1992) **Measure theory and fine properties of functions**, CRC Press, Inc.

Goodman J.W. (2000) **Statistical Optics**, JOHN WILEY & SONS.

Green M.L. (2002) **Statistics of Images, the TV Algorithm of Rudin-Osher-Fatemi for Image Denoising and an Improved Denoising Algorithm**, CAM Report, UCLA.

Greenberg N. L., Fukuda S., Agler D., Matsumura Y., Shiota T. and Thomas J. D. (2006) **4D Ultrasound Quantification of LV Function and Valvular Pathology**, Journal of IEEE.

Hogg R.V., McKean J.W. and Craig A.T. (2005) **Introduction to Mathematical Statistics**, PEARSON Prentice Hall.

Kreyszig E. (1970) **Introductory Mathematical Statistics**, JOHN WILEY and SONS, Inc.

Kreyszig E. (1988) **Introductory Functional Analysis with Applications**, JOHN WILEY and SONS, Inc.

Le T., Chatrand R. and Asaki T.J. (2005) **A Variational Approach to Reconstructing Images Corrupted by Poisson Noise**, Journal of Mathematical Imaging and Vision.

Lopes A., Touzi R. and Nezry E. (1990) **Adaptative speckle filters and scene heterogeneity**, Journal of IEEE.

Pedrotti F.L. and Pedrotti L.S. (1993) **Intoduction to Optics**, Prentice-Hall.

Rudin L.I., Osher S. and Fatemi E. (1992) **Nonlinear Total Variation Based Noise Removal Algorithms**, Journal of Physica D.

Wade W.R. (1999) **An Introduction to Analysis**, Prentice-Hall.

Watkins D. (1991) **Fundamentals of Matrix Computations**, JOHN WILEY and SONS, Inc.

Wataganara T., Sutanthavibool A. and Limwongse C. (2006) **Real-Time Three Dimensional Sonographic Features of an Early Third Trimester Fetus with Achondrogenesis**, Journal of Med Assoc Thai.

Wikipedia. **Gradient descent** [On-line]. Available: http://en.wikipedia.org/wiki/Gradient_descent.

Wikipedia. **Medical ultrasonography** [On-line]. Available: http://en.wikipedia.org/wiki/Medical_ultrasonography.

APPENDICES

APPENDIX A

SPECKLE FILTERS IN RADAR IMAGING

speckle noise is present not only in ultrasound imagez, but also in the radar images. There are many researches dealing with speckle filter in the radar images. For example

1. **Frost et al. filter (1982)**

   The speckle noisy image can be represented by the uncorrelated multiplicative model:

   $$\widetilde{u}(x,y) = R(x,y) \cdot n(x,y), \tag{A.1}$$

   where (x,y) are the spatial coordinate, $\widetilde{u}(x,y)$ is the observed image, $n(x,y)$ is the white noise and $R(x,y)$ is an *autoregressive process*[*] with an autocorrelation function $R_R(x,y)$:

   $$R_R(x,y) = \sigma_R^2 e^{-a\|(x,y)\|} + \overline{R}^2,$$

   where $\overline{R}(x,y)$ is the image local mean, σ_R^2 is the image local variance, a is the autocorrelation parameter and $\|(x,y)\|$ is the norm of (x,y).

   There are several methods used for reducing the speckle noise which follow the above noise model and the method for the *minimum mean square error*[†]

[*] **Autoregressive process** is a model which presents that the observed value x_t is determined by the values of $x_{t-1}, ..., x_{t-p}$ or the p-observed values before x_t. The autoregressive process can be written by

$$x_t = c + \sigma_{i=1}^{p} \varphi_i x_{i-t} + \varepsilon_t,$$

where c is a constant, φ_i is called autocorrelation parameter and ε_t is error of process.

[†] The mean square error of the parameter u to approximate the parameter $\widetilde{u}$ is given by the the mean or expected value of $(u - \widetilde{u})^2$.

(MMSE).

Frost presented the MMSE filter $m(x, y)$ which is given by

$$m(x, y) = K_2 \alpha e^{-\alpha \|(x,y)\|},$$

where K_2 is a constant and

$$\alpha^2 = a^2 + 2a \cdot \frac{\left(\frac{\overline{n}}{\sigma_n}\right)^2}{\left(1 + \left(\frac{\overline{R}}{\sigma_R}\right)^2\right)},$$

where $\overline{n}$ is the mean of the noise and σ_n is the variance of the noise.

A simplification of the above filter leads to the loss of the parameter a. The simplifier expression $\alpha^2 = K \cdot C_{\widetilde{u}}^2$ is used. Hence the Frost filter is given by

$$m(x, y) = K_1 e^{\left(-KC_{\widetilde{u}}^2(x_0,y_0)\|(x,y)\|\right)},$$

where K_1 is the filter parameter, $C_{\widetilde{u}}^2(x_0, y_0)$ is computed over an area centered at (x_0, y_0) and K_1 is a normalizing constant which includes α.

2. **Lee filter (1980)**

The noisy image can be represented by an additive model also.

$$\widetilde{u}(x, y) = u(x, y) + n(x, y), \tag{A.2}$$

where $\widetilde{u}$ is the considered image, u is a noiseless image, n is the additive noise.

Then, the linear MMSE filter is given by the following function $\widehat{u}(x, y)$,

$$\widehat{u}(x, y) = \overline{\widetilde{u}}(x, y) + (\widetilde{u}(x, y) - \overline{\widetilde{u}}(x, y)) \left(\frac{\sigma_u^2(x, y)}{\sigma_u^2(x, y) + \sigma_n^2(x, y)}\right), \tag{A.3}$$

where $\overline{\widetilde{u}}$ is the mean of $\widetilde{u}$, σ_u^2 and σ_n^2 is the variance of u and n respectively.

The Lee filter applies this linear MMSE filter for considering the multiplicative noise. It can be described in the form of weighted sum of the observed image and mean values:

$$\widehat{u}(x,y) = \widetilde{u}(x,y) \cdot W(x,y) + \overline{\widetilde{u}}(x,y) \cdot (1 - W(x,y)), \tag{A.4}$$

where the weight function W is given by

$$W(x,y) = 1 - \frac{C_n^2}{C_{\widetilde{u}}^2(x,y)},$$

where $C_n^2 = \dfrac{\sigma_n}{\overline{n}}$ and $C_{\widetilde{u}}^2 = \dfrac{\sigma_{\widetilde{u}}}{\overline{\widetilde{u}}}$ are the noise and image variation coefficients respectively.

3. **Kuan et al. filter (1985)**

Kuan presented a filter to deal which linear MMSE filter for considering of the multiplicative noise just as the Lee filter. This filter is written by (A.4) with the weight function

$$W(x,y) = \frac{1 - \frac{C_n^2}{C_{\widetilde{u}}^2(x,y)}}{1 + C_u^2}.$$

4. Homomorphic Filter

Arsenals (1984) and Yan and Chen (1986) also used the multiplicative speckle noise model shown in equation (A.1). A logarithmic transformation is performed to obtain the additive noise model by

$$\ln \widetilde{u}(x,y) = \ln R(x,y) + \ln n(x,y).$$

Then, the linear MMSE filter in equation (A.3) is used for this noise model.

APPENDIX B

PROTOTYPE SOFTWARE

B.1 Prototype Software

The Prototype software is developed for the experiment. It is implemented in the *Pascal language* on *Borland Delphi* version 6. In order to work with the video files, the additional library *Mitov software VideoLab* version 3.1 is installed.

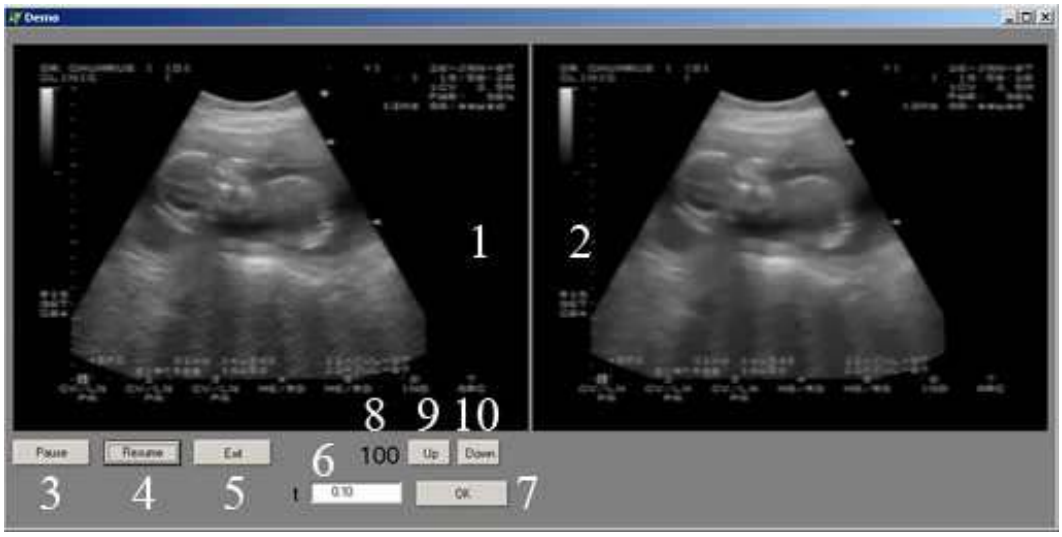


Figure B.1 The figure of prototype software and its components.

As show in figure B.1, the software components are as follows;

1. **Original video displayer**

   The original video is shown on the left displayer.

2. **Reconstructed video displayer**

   The reconstructed video is shown on the right displayer.

3. **Pause button**

   The video is paused if this button is clicked.

4. **Resume button**

   The paused video is resumed if this button is clicked.

5. **Exit button**

   This button is used for the program closing.

6. **Step size text field**

   The step size is filled in the text field and then the OK button is used for the activation.

7. **OK button**

   This button is used for activating of the step size in text field.

8. **Iterative label**

   The number of iterative loops is labeled in this component.

9. **Up button**

   When the increasing of the reconstructed iteration loops is required, this button is used.

10. **Down button**

    Converse from Up button, if the decreasing of the reconstructed iteration loops is required, this button is used.

B.2 Source Code

Source code is composted by two classes.

1. **Main class**.

   This part is used for initialization all of the modules, components and variable of the form. This class is the first part working when the program is execute and run.

```
program Project1;

uses
  Forms,
  Unit1 in 'Unit1.pas' {Form1};

begin
  Application.Initialize;
  Application.CreateForm(TForm1, Form1);
  Application.Run;
end.
```

2. **Computational class**.

   The computational part dealing with the numerical scheme include the display part is implemented in this class.

```
unit Unit1;

interface

uses
  Windows, Messages, SysUtils, Variants,
```

```
  Classes, Graphics, Controls, Forms,
  Dialogs, VLCommonDisplay, VLDSImageDisplay,
  VLDSVideoPlayer, SLScope, VLSinkFilter, VLHistogram,
  VLCommonFilter, VLGenericFilter, StdCtrls,
  ComCtrls, Buttons, VLImageDisplay;

{component declarations}
type
    TForm1 = class(TForm)
    VLDSVideoPlayer1: TVLDSVideoPlayer;
    VLDSImageDisplay1: TVLDSImageDisplay;
    VLDSImageDisplay2: TVLDSImageDisplay;
    VLGenericFilter1: TVLGenericFilter;
    PlayButton: TButton;
    PauseButton: TButton;
    Label2: TLabel;
    BitBtn1: TBitBtn;
    BitBtn2: TBitBtn;
    BitBtn3: TBitBtn;
    Label3: TLabel;
    Edit1: TEdit;
    Button1: TButton;
    procedure VLGenericFilter1ProcessData(Sender: TObject;
      InBuffer: IVLImageBuffer; var OutBuffer: IVLImageBuffer;
      var SendOutputData: Boolean);
    procedure PlayButtonClick(Sender: TObject);
```

```
    procedure PauseButtonClick(Sender: TObject);
    procedure FormCreate(Sender: TObject);
    procedure BitBtn1Click(Sender: TObject);
    procedure BitBtn2Click(Sender: TObject);
    procedure BitBtn3Click(Sender: TObject);
    procedure FormCloseQuery(Sender: TObject;
      var CanClose: Boolean);
    procedure Button1Click(Sender: TObject);

  private
    { Private declarations }
  public
    { Public declarations }
  end;

{constant declarations}
const
  p = 0.1;
  err_thres = 0.0001;
  maxloop = 500;

{variable declarations}
var
  Form1 : TForm1;
  U0, U, UTemp : Array of Array of real;
  t,temp,rn : real;
```

```
  Loop : Integer;
  St   : String;

implementation

{computational and displayed procedure}
procedure TForm1.VLGenericFilter1ProcessData(Sender: TObject;
InBuffer: IVLImageBuffer; var OutBuffer: IVLImageBuffer;
var SendOutputData: Boolean);

{variable declarations}
var
    InDataAccess : IVLImageDataAccess;
    OutDataAccess : IVLImageDataAccess;
    i, j ,k, m, n: Integer;
    Dx, Dy, DX1, DX2, DY1, DY2, E, sume : real;
    um1, um2, um3, um4, ui1, ui2, ui3, ui4 : real;
    un1, un2, un3, un4, uj1, uj2, uj3, uj4 : real;
    sm2, sm3, si2, si3 : real;
    sn2, sn3, sj2, sj3 : real;
    mm, mi, mn, mj : real;

  {get the image data}
  begin
    InDataAccess := InBuffer.Data();
    OutDataAccess := OutBuffer.Data();
```

```
SetLength(U0,InDataAccess.Width,InDataAccess.Height);
SetLength(U,InDataAccess.Width,InDataAccess.Height);
SetLength(UTemp,InDataAccess.Width,InDataAccess.Height);

  {gray scaling transformation}
  for i := 0 to InDataAccess.Width-1 do
  begin
    for j := 0 to InDataAccess.Height-1 do
    U0[i,j] := Round(0.33*InDataAccess.Red[i,j]
               +0.33*InDataAccess.Green[i,j]
               +0.33*InDataAccess.Blue[i,j]);
  end;{end for i}

  {initialization of array}
  for i := 0 to InDataAccess.Width-1 do
  begin
    for j := 0 to InDataAccess.Height-1 do
    U[i,j] := U0[i,j];
  end;{end for i}

  {numerical part}
  k := 0;
  while (k<Loop) do
  begin
        for i := 0 to InDataAccess.Width-1 do
        begin
```

```
        for j := 0 to InDataAccess.Height-1 do
        UTemp[i,j] := U[i,j];
    end;{end for i}

    for i := 1 to InDataAccess.Width-2 do
    begin
      for j := 1 to InDataAccess.Height-2 do
      begin
      {DX1**********************************}
      m := i-1;
      um1 := UTemp[m+1,j]-UTemp[m,j];
      um2 := UTemp[m,j+1]-UTemp[m,j];
      um3 := UTemp[m,j]-UTemp[m,j-1];

      {sign um2}
      if um2 > 0 then sm2 := 1
else if um2 = 0 then sm2 := 0
else                 sm2 := -1;
      {sign um3}
      if um3 > 0 then sm3 := 1
else if um3 = 0 then sm3 := 0
else                 sm3 := -1;
      {min m}
      if abs(um2) < abs(um3) then mm := abs(um2)
                             else mm := abs(um3);
```

```
      um4 := ((sm2+sm3)/2)*mm;
      temp := (um1*um1)+(um4*um4);
      if abs(temp)<err_thres then Dx1 := 0
      else DX1 := um1/Sqrt(temp);
      {end DX1*****************************}

      {DX2*********************************}
      ui1 := UTemp[i+1,j]-UTemp[i,j];
      ui2 := UTemp[i,j+1]-UTemp[i,j];
      ui3 := UTemp[i,j]-UTemp[i,j-1];

      {sign ui2}
      if ui2 > 0 then si2 := 1
else if ui2 = 0 then si2 := 0
else                 si2 := -1;

      {sign ui3}
      if ui3 > 0 then si3 := 1
else if ui3 = 0 then si3 := 0
else                 si3 := -1;

      {min i}
      if abs(ui2) < abs(ui3) then mi := abs(ui2)
                             else mi := abs(ui3);

      ui4 := ((si2+si3)/2)*mi;
```

```
      temp := (ui1*ui1)+(ui4*ui4);
      if abs(temp)<err_thres then Dx2 := 0
      else DX2 := ui1/Sqrt(temp);
      {end DX2*****************************}

      Dx := DX2-DX1;

      {DY1*********************************}
      n := j-1;
      un1 := UTemp[i,n+1]-UTemp[i,n];
      un2 := UTemp[i+1,n]-UTemp[i,n];
      un3 := UTemp[i,n]-UTemp[i-1,n];

      {sign um2}
      if un2 > 0 then sn2 := 1
 else if un2 = 0 then sn2 := 0
 else                 sn2 := -1;
      {sign um3}
      if un3 > 0 then sn3 := 1
 else if un3 = 0 then sn3 := 0
 else                 sn3 := -1;

      {min n}
      if abs(un2) < abs(un3) then mn := abs(un2)
                             else mn := abs(un3);
```

```
      un4 := ((sn2+sn3)/2)*mn;
      temp := (un1*un1)+(un4*un4);
      if abs(temp)<err_thres then Dy1 := 0
      else DY1 := un1/Sqrt(temp);
      {end DY1*****************************}

      {DY2*********************************}
      uj1 := UTemp[i,j+1]-UTemp[i,j];
      uj2 := UTemp[i+1,j]-UTemp[i,j];
      uj3 := UTemp[i,j]-UTemp[i-1,j];

      {sign uj2}
      if uj2 > 0 then sj2 := 1
else if uj2 = 0 then sj2 := 0
else                 sj2 := -1;
      {sign um3}
      if uj3 > 0 then sj3 := 1
else if uj3 = 0 then sj3 := 0
else                 sj3 := -1;

      {min j}
      if abs(uj2) < abs(uj3) then mj := abs(uj2)
                             else mj := abs(uj3);

      uj4 := ((sj2+sj3)/2)*mj;
```

```
        temp := (uj1*uj1)+(uj4*uj4);
        if abs(temp)<err_thres then Dy2 := 0
        else DY2 := uj1/Sqrt(temp);
        {end DY1*****************************}

        Dy := DY2-DY1;

        if abs(Utemp[i,j])<err_thres then E := 0
        else
        E := (2/(Utemp[i,j]*Utemp[i,j]*Utemp[i,j]))*
             ((U0[i,j]*U0[i,j])-
             (Utemp[i,j]*Utemp[i,j]));;
        U[i,j] := Utemp[i,j]+t*((Dx+Dy)/2+E);
        if U[i,j]<0 then U[i,j]:=0;
        end;{end for j}
      end;{end for i}
      k := k+1;
end;

{displayed part}
for j := 0 to InDataAccess.Height-1 do
begin
  for i := 0 to InDataAccess.Width-1 do
  begin
          OutDataAccess.Red[i,j] := Round(U[i,j]);
          OutDataAccess.Green[i,j] := Round(U[i,j]);
```

```
                OutDataAccess.Blue[i,j] := Round(U[i,j]);
        end;{end for i}
    end;{end for j}

end;{procedure}

{Resumed procedure}
procedure TForm1.PlayButtonClick(Sender: TObject);
begin
VLDSVideoPlayer1.Resume;
end;

{Paused procedure}
procedure TForm1.PauseButtonClick(Sender: TObject);
begin
VLDSVideoPlayer1.Pause;
end;

{Form variable initialization}
procedure TForm1.FormCreate(Sender: TObject);
begin
        Loop := 7;
        str(loop,st);
        Label2.Caption := st;
        t := 1;
        str(t:10:2,st);
```

```
        edit1.text := st;
end;

{Loop increasing procedure}
procedure TForm1.BitBtn1Click(Sender: TObject);
begin
     If Loop<maxloop then
     begin
        Loop := Loop+1;
        str(loop,st);
        Label2.Caption := St;
     end;
end;

{Loop decreasing procedure}
procedure TForm1.BitBtn2Click(Sender: TObject);
begin
     If Loop>0 then
     begin
        Loop := Loop-1;
        str(loop,st);
        Label2.Caption := St;
     end;
end;

{Form closed procedure}
```

```
procedure TForm1.BitBtn3Click(Sender: TObject);
begin
        Form1.Close;
end;

{Object Destroyed procedure}
procedure TForm1.FormCloseQuery(Sender:
TObject; var CanClose: Boolean);
begin
   VLGenericFilter1.Destroy;
   VLDSVideoPlayer1.Destroy;
end;

{Step size controller}
procedure TForm1.Button1Click(Sender: TObject);
var       code : integer;
          temp : real;
begin
     st := edit1.text;
     val(st,temp,code);
     if code=0 then t := temp;
     str(t:0:2,st);
     edit1.text := st;
end;

end.
```

CURRICULUM VITAE

FIRST NAME: Watchirawoot LAST NAME: Seekot

GENDER: Male NATIONALITY: Thai DATE OF BIRTH: June 22, 1983

EDUCATION BACKGROUND:

- Bachelor of Science in Computer Science (Second Class Honours),
  May 26, 2002 - March 29, 2006,
  Khonkaen University, Khonkaen, Thailand.

WORK EXPERIENCES:

- Teaching Assistant in Calculus I, II and III, School of Mathematics, Suranaree University of Technology.

- Teaching Assistant in Business Mathematics I and II, School of Management Technology, Suranaree University of Technology.

PUBLICATION:

- Seekot, W. and Tanthanuch, J. (In Press). **ULTRASOUND IMAGE ENHANCEMENT BY MEANS OF A VARIATIONAL APPROACH**, Proceedings of 11^{th} National Graduate Conference, Valaya Alongkorn Rajabhat University.

SCHOLARSHIPS AND AWARDS:

- Scholarship for the promising graduate students, academic year 2006 - 2007, Suranaree University of Technology.

- Good oral presentation award, 11^{th} National Graduate Conference, December 17 - 18, 2008, Valaya Alongkorn Rajabhat University.